Doctoral Dissertation

Synthesis of Polyaniline/Metal Nanoparticles Hybrids and their Properties

Tadayuki Isaji

January 2015

Department of Applied Chemistry

Graduate School of Engineering,

Osaka University

Doctoral Dissertation

Synthesis of Polyaniline/Metal Nanoparticles Hybrids and their Properties

（ポリアニリン／金属ナノ粒子複合体の合成とその特性）

Tadayuki Isaji

January 2015

Department of Applied Chemistry

Graduate School of Engineering,

Osaka University

Preface

The studies presented in this thesis were performed under the guidance of Professor Toshikazu Hirao, Department of Applied Chemistry, Graduate School of Engineering, Osaka University during 2012-2015.

The objects of this thesis are studies on synthesis of polyaniline/metal nanoparticle hybrids and their properties.

The author hopes that this basic work described in this thesis contributes to the further development of the utility of conductive polymers.

Tadayuki Isaji

Department of Applied Chemistry

Graduate School of Engineering

Osaka University

Suita, Osaka

Japan

January, 2015

Contents

General Introduction

Electroconductive and π-conjugated polymers have attracted interest owing to their various electrical and optical properties, which are caused by the movement of π-electrons in their structure. Furthermore, π-conjugated polymers have excellent features compared to inorganic materials from the viewpoints of weight, workability, and moldability. Therefore, various electroconductive polymers, such as those shown in Figure 1, have been developed.

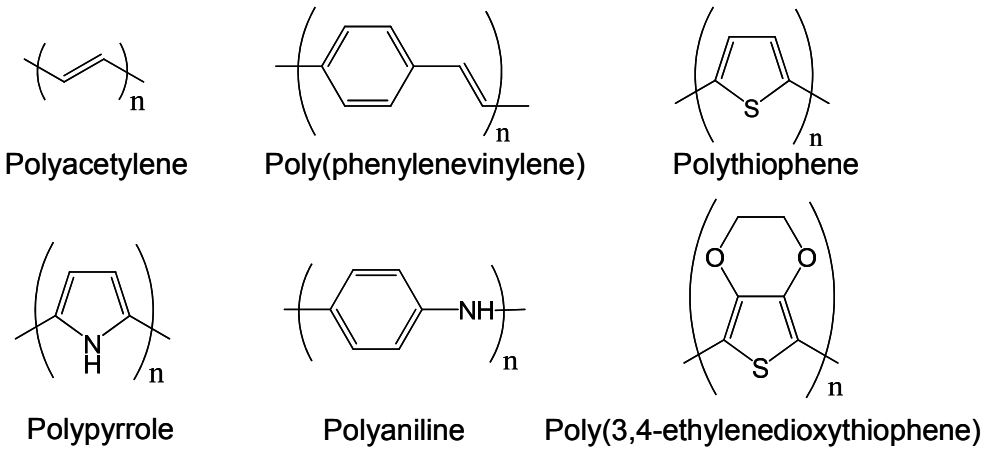

Figure 1. Various electroconductive polymers.

Polyaniline (PAni) is present in various redox states, as shown in Figure 2, and can have high conductivity. Therefore, applications utilizing its conductivity and redox properties are expected.[1] PAni can coordinate to metals through its quinonediimine nitrogen sites, which permit electronic interaction with a coordinated metal. Such PAni/metal composites have been used as catalysts, sensors, and electrodes.[2-5]

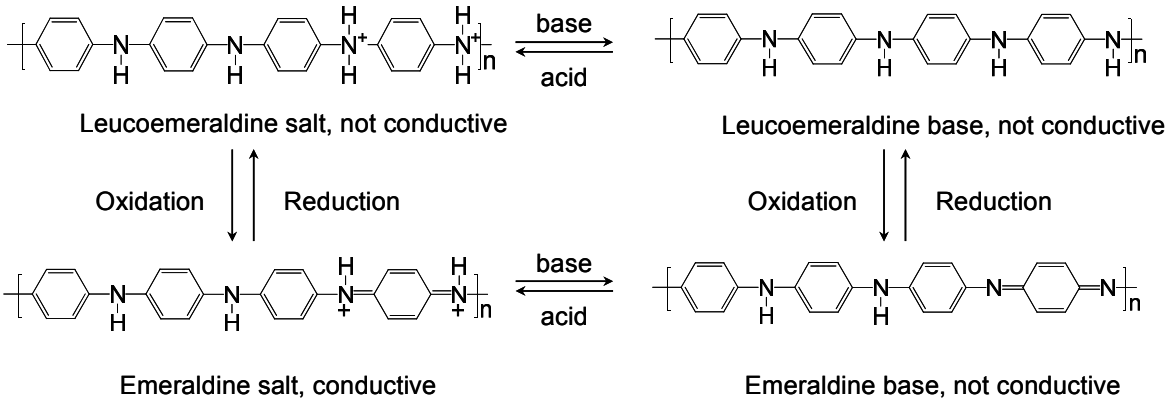

Figure 2. Redox states of PAni.

The synthesis of PAni complexes with various transition metals, and their catalytic function and redox properties, have been studied in our laboratory.[6, 7] For example, the use of a PAni/Pd^{2+} complex in the Wacker oxidation of alkenes has been reported.[8] Furthermore, the syntheses of PAni/Pd nanoparticles (NPs) hybrids via the direct reduction method,[9] the template method,[10] and the ligand exchange method[11] have also been studied. The use of PAni/Pd NPs hybrids in the oxidative coupling reaction of 2,6-di-*t*-butylphenol was also successful. We also developed hybrid catalysts consisting of water-soluble polyaniline sulfonic acid containing Au NPs.[12, 13] These hybrid catalysts are useful in the dehydrogenative oxidation of alcohols and amines, in which molecular oxygen is the terminal oxidizing agent. In this reaction, polyaniline sulfonic acid works as a redox mediator (Figure 3).[12, 13a] The synthesis and evaluation of PAni/M NPs hybrids have been studied in our laboratory, but thus far the metal species has been limited to Pd.

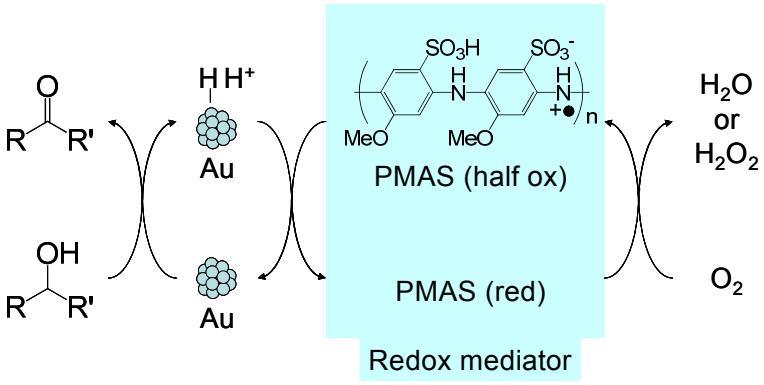

Figure 3. Oxidation reaction using poly(2-methoxyaniline-5-sulfonic acid) (PMAS)/Au NPs hybrids.

The generation of active oxygen or hydrogen peroxide in water is known to be an effective method for sterilizing water containing bacteria and other microorganisms.[14] The generation of active oxygen or related species for this purpose, by the electrochemical reduction of oxygen dissolved in water, has been reported.[15] Some reports have described methods using PAni or PAni derivatives.[16-18] For an electrode catalyst using PAni, the mechanism for generating active oxygen species has been proposed as follows: (1) PAni is reduced on the cathode electrode, then (2) the reduced PAni is reoxidized by molecular oxygen in water, resulting in the generation of a superoxide anion radical (Figure 4).

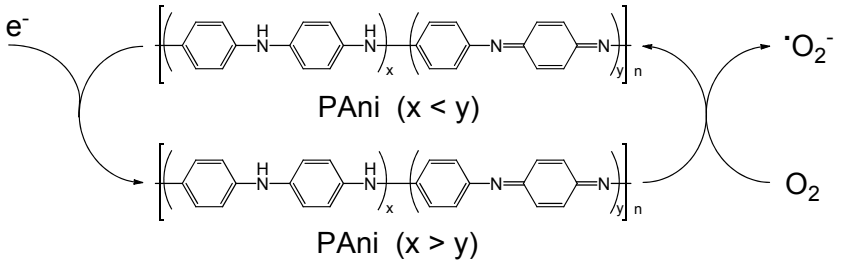

Figure 4. Schematic catalytic cycle for the generation of active oxygen species on the electrode with PAni.

This catalytic redox cycle of PAni would facilitate continuous generation of the superoxide radical anion. PAni/M NPs hybrids (where the metal was Pt) have also been studied as electrode catalysts for the oxygen reduction reaction in fuel cells under acidic conditions. [19-23] Under these conditions, oxygen would be reduced to water. However, the generation of active oxygen species under acidic conditions has not been investigated, because, from an environmental point of view, acidic conditions are undesirable for antibacterial use.

To study the catalytic generation of active oxygen species, the synthesis of hybrids of many metal species with PAni was required. Group 10 and 11 elements, which were expected to show catalytic activity, were selected as the metal species. Because there is an electronic interaction between PAni and the M NPs in the hybrids, the repetition durability and redox properties will change when different metals are used as a redox electrode. Therefore, one of the purposes of this study was to investigate the effect of metal species hybridized with PAni for their conductivity and catalytic properties for active oxygen generation. The syntheses of PAni/M NPs hybrids by either the ligand exchange method (Scheme 1a) or the template method (Scheme 1b) were also studied. Finally, the electrical properties and the generation of active oxygen species in

neutral water were investigated by using proton-doped PAni/M NPs (H^+-PAni/M NPs) hybrids (Scheme 1c).

(a) Ligand exchange method

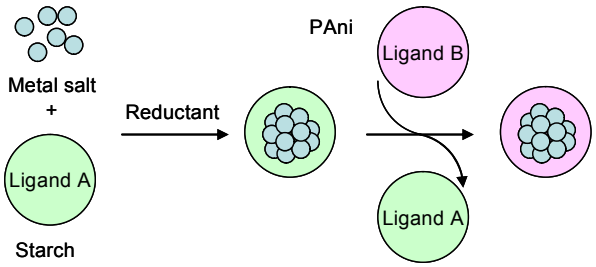

(b) Template method

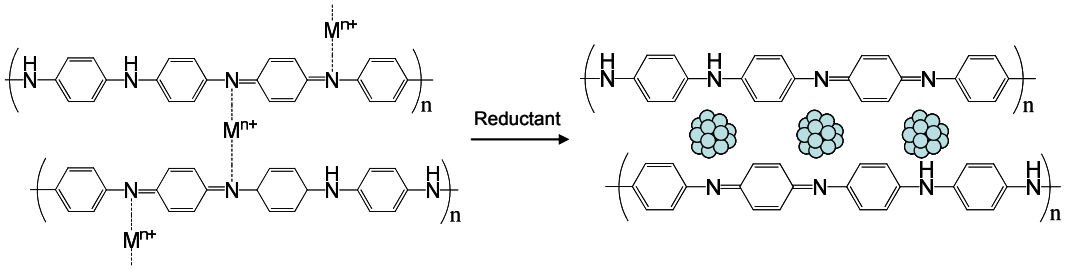

(c) Generation of active oxygen species

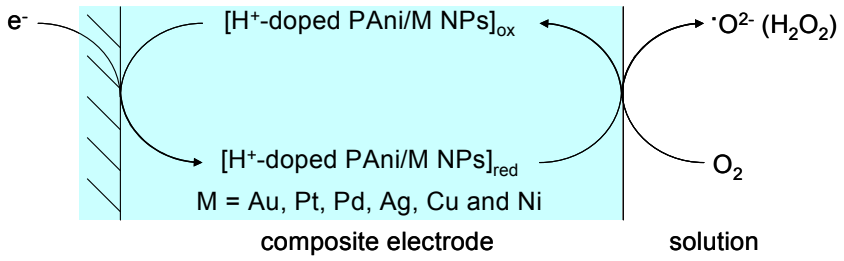

Scheme 1. Schematic of the preparation of PAni/M NPs hybridws by (a) ligand exchange method and (b) template method, and (c) generation of active oxygen species by H^+-PAni/M NPs hybrids.

This thesis consists of three chapters:

Chapter 1 describes the synthesis of PAni/M NPs hybrids (M = Au, Pt, and Ag) via the ligand exchange method. In this method, after the synthesis of starch/M NPs, the sacrificial ligand was exchanged with PAni.

Chapter 2 describes the synthesis of PAni/M NPs hybrids (M = Au, Pt, Pd, Ag, Cu, and Ni) via the template method. In this method, PAni/M^{n+} complexes were synthesized, followed by the reduction of M^{n+} using a reductant to yield the corresponding PAni/M NPs hybrids.

Chapter 3 describes the electrical properties of PAni/M NPs hybrids and PAni/M^{n+} complexes (M = Au, Pt, Pd, Ag, Cu, and Ni), and the generation of active oxygen in water by using the synthesized PAni/M NPs hybrids (M = Au, Pt, Pd, Ag, Cu, and Ni).

References

1. G. Ćirić-Marjanović, *Synth. Met.* **2013**, *177*, 1-47.
2. R. J. Tseng, J. Huang, J. Ouyang, R. B. Kaner, Y. Yang, *Nano Lett.* **2005**, 1077-1080.
3. M. Riskin, B. Basnar, Y. Huang, I. Willner, *Adv. Mater.* **2007**, *19*, 2691-2695.
4. B. J. Gallon, R. W. Kojima, R. B. Kaner, P. L. Diaconescu, *Angew. Chem., Int. Ed.* **2007**, *46*, 7251-7254.
5. D. Zhai, B. Liu, Y. Shi, L. Pan, Y. Wang, W. Li, R. Zhang, G. Yu, *ACS Nano* **2013**, *7*, 3540-3546.
6. T. Hirao, *Coord. Chem. Rev.* **2002**, *226*, 81-91.
7. T. Moriuchi, T. Hirao, *Acc. Chem. Res.* **2012**, *45*, 347-360.
8. T. Hirao, M. Higuchi, B. Hatano, I. Ikeda, *Tetrahedron Lett.* **1995**, *36*, 5925-5928.
9. T. Amaya, D. Saio, T. Hirao, *Macromol. Symp.* **2008**, *270*, 88-94.
10. T. Amaya, D. Saio, T. Hirao, *Tetrahedron Lett.* **2007**, *48*, 2729-2732.
11. D. Saio, T. Amaya, T. Hirao, *J. Inorg. Organomet. Polym*. **2009**, *19*, 79-84.
12. D. Saio, T. Amaya, T. Hirao, *Adv. Synth. Catal.* **2010**, *352*, 2177-2180.
13. (a) T. Amaya, T. Ito, Y. Inada, D. Saio, T. Hirao, *Tetrahedron Lett.* **2012**, *53*, 6144-6147, (b) T. Amaya, T. Ito, T. Hirao, *Heterocycles* **2012**, *86*, 927-932, (c) T. Amaya, T. Ito, T. Hirao, *Tetrahedron Lett.* **2013**, *54*, 2409-2411.
14. E. Cabiscol, J. Tamarit, J. Ros*, Internatl. Microbiol.* **2000**, *3*, 3-8.
15. A. Kraft, *Platinum Metals Rev.* **2008**, *52*, 177-185.
16. N. Kawashima, M. Takamatsu, K. Morita, *Colloids and Surfaces B: Biointerfaces* **1998**, *11*, 297-299.
17. H. Ono, T. Okajima, F. Matsumoto, T. Oritani, A. Shimizu, M. Takahashi, T. Ohsaka, *Electrochemistry* **2001**, *69*, 953-955.
18. N. Ohki, S. Uesugi, K. Murayama, F. Matsumoto, N. Koura, T. Okajima, T. Ohsaka, *Electrochemistry* **2002**, *70*, 23-29.
19. H. Nakano, Y. Tachibana, S. Kuwabata, *Electrochimica Acta* **2004**, *50*, 749-754.
20. A. Kongkanand, S. Kuwabata, *J. Phys. Chem. B* **2005**, *109*, 23190-23195.
21. V. G. Khomenko, V. Z. Barsukov, A. S. Katashinskii, *Electrochimica Acta* **2005**, *50*, 1675-1683.
22. A. Drelinkiewicz, A. Zięba, J. W. Sobczak, M. Bonarowska, Z. Karpiński, A. Waksmundzka-Góra, J. Stejskal, *React. Funct. Polym.* **2009**, *69*, 630-642.
23. A. Morozan, B. Jousselme, S. Palacin, *Energy Environ. Sci.* **2011**, *4*, 1238-1254.

Chapter 1: Synthesis of polyaniline/metal nanoparticles hybrids via ligand exchange method(1)

Introduction

PAni/Pd NPs have been successfully synthesized by the ligand exchange method in our laboratory.[1] In this method, starch/M NPs are synthesized by reduction of a mixture of starch and metal salts in the first step. Thereafter, the starch ligand is replaced with PAni in the second step (Scheme 2). It was thought as an ideal method for the synthesis of hybrids because damage to the PAni by the reductant could be avoided.

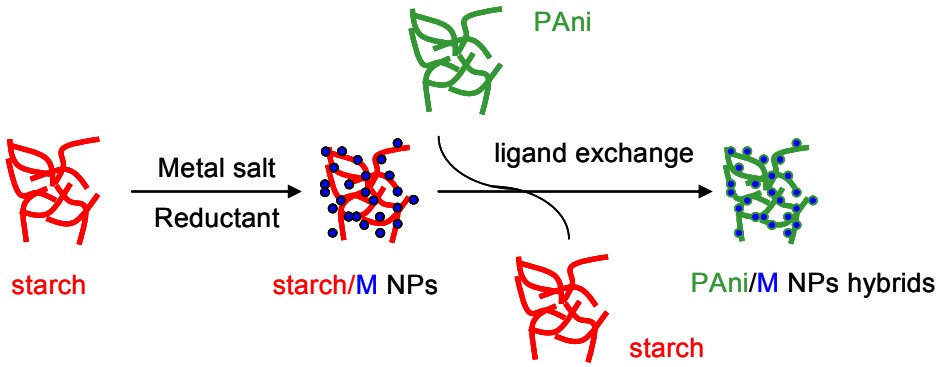

Scheme 2. Schematic of the preparation of PAni/M NPs hybrids via ligand exchange method.

Here, I report the synthesis of starch/M NPs (M = Au, Pt, and Ag) and the synthesis of PAni/M NPs hybrids (M = Au, Pt, and Ag) via ligand exchange with starch/M NPs.

Results and discussion

Synthesis of starch/M NPs

Au, Pt, and Ag were selected as the metal species, which were expected to improve the electrical and catalytic properties of the PAni/M NPs hybrids. Starch/M NPs (M = Au, Pt, and Ag) were produced as follows (Scheme 3).

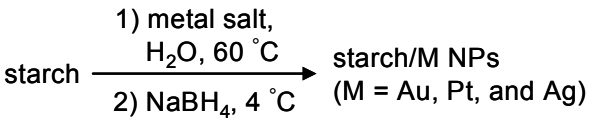

Scheme 3. The synthesis of starch/M NPs (M = Au, Pt, and Ag).

Table 1. The used metal salts in synthesis of starch/M NPs.

Metal	M^{n+}
Au	$NaAuCl_4 \cdot 2H_2O$
Pt	$Na_2PtCl_6 \cdot 6H_2O$
Ag	$AgNO_3$

A mixture of starch and metal salts in water, as listed in Table 1, was sonicated and stirred. The transparent solutions obtained all had a light yellow color. Then, an aqueous solution of $NaBH_4$ was added dropwise to the solutions. After stirring, the excess $NaBH_4$ was quenched by adding 1 M HCl solution. Anionic and cationic ion exchange resins removed the remaining ions, such as Na^+, Cl^-, and NO^{3-}. The color of all of the samples was then a transparent dark brown. Figure 5 shows TEM images of the starch/M NPs (M = Au, Pt, and Ag). Small particles (in the range of 2-3 nm) were observed.

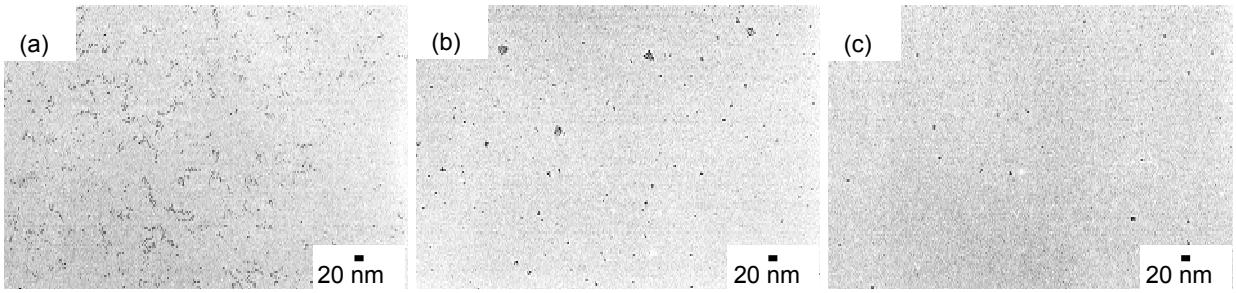

Figure 5. TEM images of (a) starch/Au NPs, (b) starch/Pt NPs, and (c) starch/Ag NPs.

Synthesis of PAni/M NPs hybrids

Using the starch/M NPs (M = Au, Pt, and Ag), ligand exchanges from starch to PAni were carried out (Scheme 4).

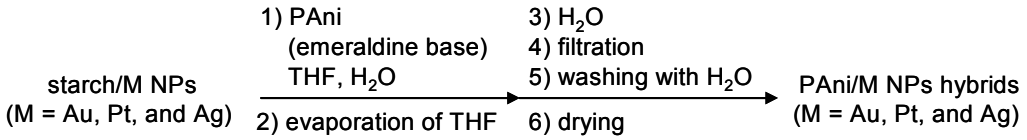

Scheme 4. The synthesis of PAni/M NPs hybrids (M = Au, Pt, and Ag).

Aqueous solutions of starch/M NPs (M = Au, Pt, and Ag) were added dropwise to THF solutions of PAni (emeraldine base). Then, the mixtures were stirred. The ratios of metals to PAni (w/w) were set to 0.1, 0.5, and 1.0 wt% by varying the amount of starch/M NPs (M = Au, Pt, and Ag) added to the PAni solutions. After stirring, the THF was removed by evaporation, and water was added to the mixtures. The mixtures were sonicated to dissolve the starch in water. Then, the mixtures were filtered and the residues were washed using hot water to yield the PAni/M NPs hybrids. The washing process was repeated until starch was not detected in the filtrate. The presence of starch was indicated by the iodine starch reaction. 450-600 mg of PAni/M NPs hybrids (M = Au, Pt, Pd, Ag, Cu, and Ni) were obtained starting from 500 mg of PAni.

Figure 6 shows TEM images of PAni/M NPs hybrids (M = Au, Pt, and Ag) (M/PAni = 1.0 wt%). For all samples, small M NPs (mainly in the range of 2-3 nm) were observed in the PAni matrix although some aggregation was observed in PAni/Pt and Ag NPs hybrids.

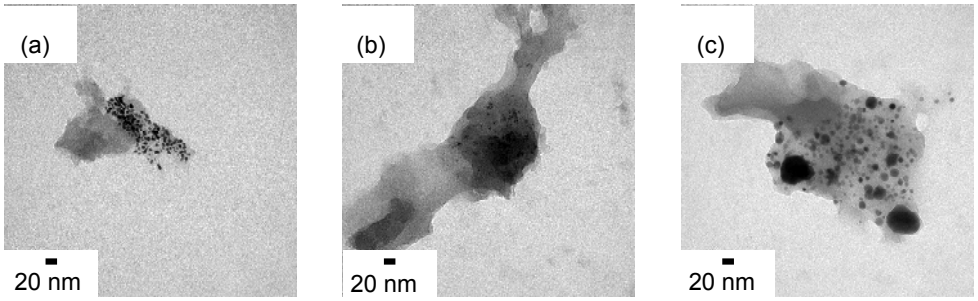

Figure 6. TEM images of (a) PAni/Au NPs hybrids (1.0 wt%), (b) PAni /Pt NPs hybrids (1.0 wt%), and (c) PAni/Ag NPs hybrids (1.0 wt%).

Figure 7 shows the IR spectra of PAni/Pt NPs hybrids (Pt/PAni = 0.1, 0.5, and 1.0 wt%) and neat PAni. All of the spectra were similar. Peaks around 1600 and 1500 cm^{-1}, which were attributable to the quinonediimine and the phenylenediamine of PAni, respectively,[2] were observed. The peak intensity ratio (quinonediimine/phenylenediamine) increased slightly after the ligand exchange in the spectra for PAni/Pt NPs hybrids (Pt/PAni = 0.5 and 1.0 wt%). This indicated the partial oxidation of the main chain structure of PAni. This phenomenon contrasts with the PAni/Pd NPs hybrids.[1] Pt has been reported to show more highly active catalysis for aerobic oxidation than Pd.[3] This oxidation reaction is catalyzed by Pt under air (molecular oxygen).

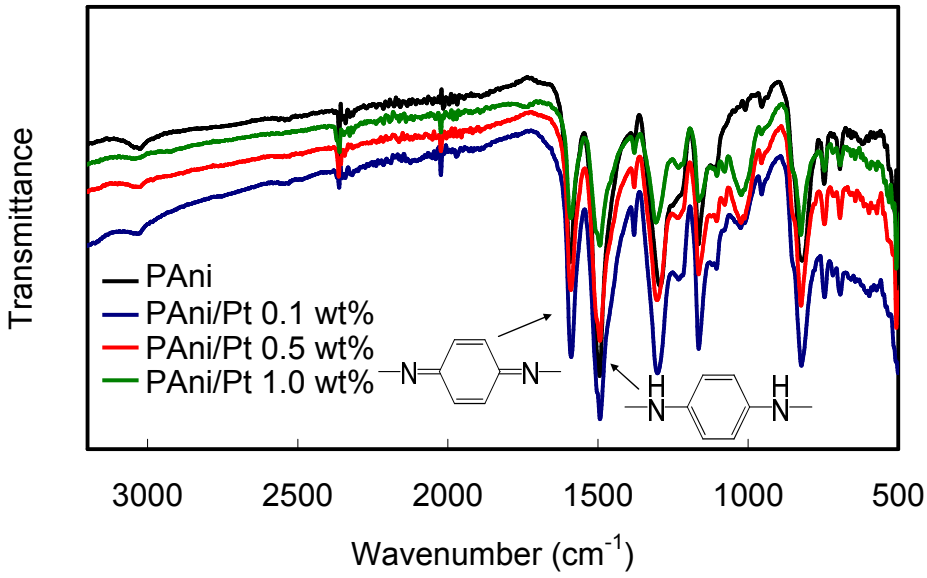

Figure 7. FT-IR spectra of PAni and PAni/Pt NPs hybrids.

Figure 8 shows the XPS spectra of PAni/Pt NPs hybrids (Pt/PAni = 1.0 wt%) for the N 1s core level. The ratio of the imine nitrogen to the amine nitrogen was 44 : 56.[2]

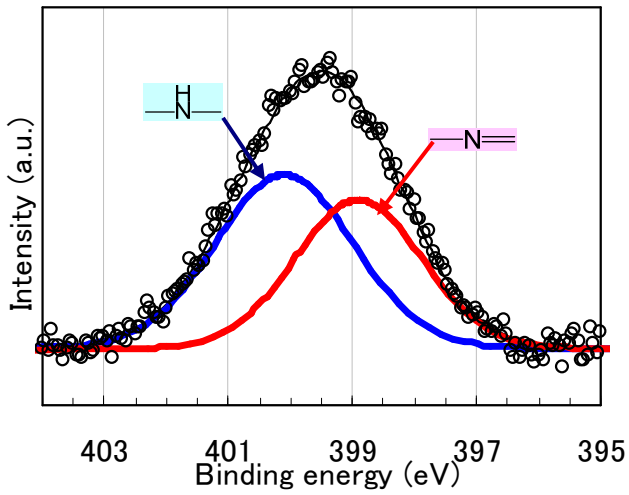

Figure 8. The XPS spectrum of PAni/Pt NPs (1.0 wt%).

Figure 9 shows the UV-Vis-NIR absorption spectra of the PAni/Pt NPs hybrids (Pt/PAni = 0.1, 0.5, and 1.0 wt%, respectively). They were also similar. The characteristic peaks were observed around 330 and 600 nm, they were attributable to the π-π* and the charge transfer transitions, respectively.[2] These are typical spectra for the emeraldine base of PAni. In all of the PAni/Pt NPs hybrids, the absorbance was decreased compared to neat PAni. The hypochromic effect was derived from intermolecular aggregation and/or an intramolecular conformation change, which could be induced by the Pt NPs. A hypochromic effect on the emeraldine base of PAni that was induced by the solvent has been observed and discussed in the literature.[4]

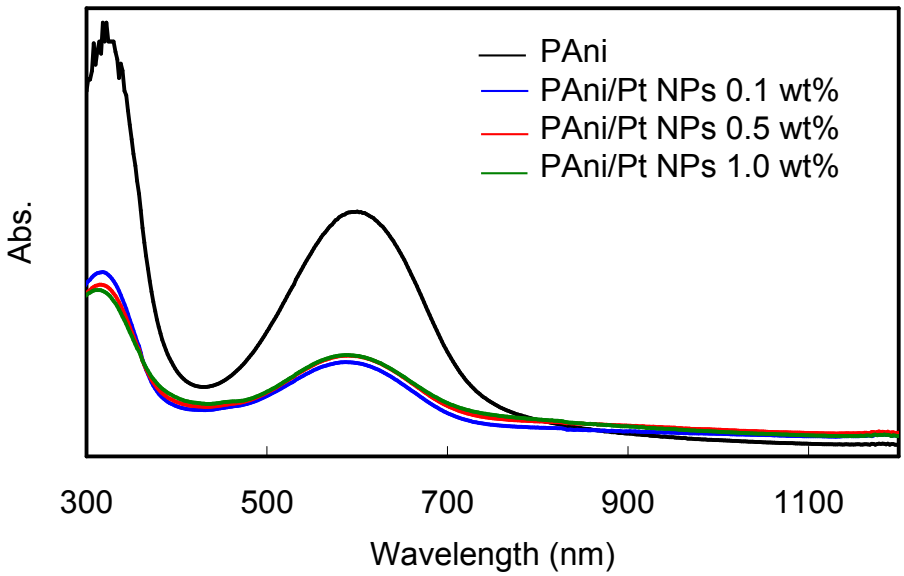

Figure 9. UV-Vis-NIR spectra (1.0×10^{-4} M based on aniline unit, THF) of PAni and PAni/Pt NPs hybrids.

Figure 10 shows the TG/DTA chart of PAni/Pt NPs hybrids (Pt/PAni = 1.0 wt%). An exothermic peak and a decrease in weight were observed at approximately 280 °C and 430-450 °C, which were caused by the combustion of starch and PAni, respectively. Washing with additional hot water to remove the starch completely was not effective, nor was washing of the powder after dispersion in THF. The starch was expected to be difficult to wash out because it was incorporated into the aggregate of PAni. However, in our previous synthesis of PAni/Pd NPs hybrids, the starch was washed out completely.[1] Here, the scale of reaction was approximately 15 times larger. This might be one of the reasons for the remaining starch.

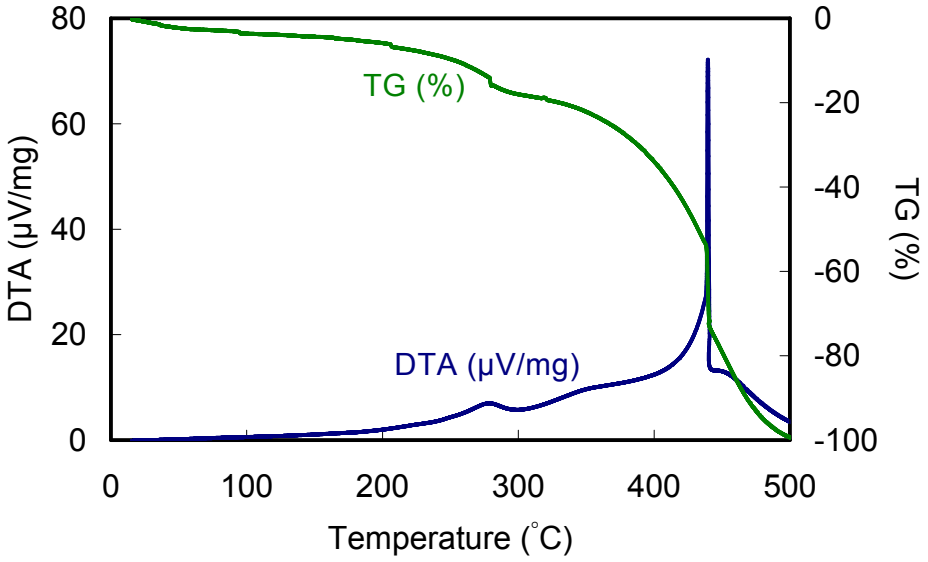

Figure 10. TG-DTA chart of PAni/Pt NPs hybrids (1.0 wt%).

Conclusion

PAni/M NPs hybrids (M = Au, Pt, and Ag) were synthesized from the corresponding precursor starch/M NPs via the ligand exchange method. The diameters

of the M NPs obtained were primarily in the range of 2-3 nm, however, some aggregation was observed in PAni/Pt and PAni/Ag NPs hybrids. Although it is difficult to remove starch completely, this procedure avoids the exposure of the redox-active polymer to the reductant, and is useful for the synthesis of PAni/M NPs hybrids.

Experimental section

Instrumentation and chemicals

All reagents were purchased from commercial sources and used without further purification. Starch (water-soluble) and $AgNO_3$ were purchased from Wako Pure Chemical Industries. PAni (emeraldine base, M_W: *ca.* 10000) was purchased from Aldrich. $NaAuCl_4 \cdot 2H_2O$ and $Na_2PtCl_6 \cdot 6H_2O$ were purchased from Kanto Chemical. TEM images were recorded on a JEOL JEM-1010. FT-IR spectra were recorded using the ATR technique with a JASCO FT/IR-4200 spectrometer. XPS spectra were recorded on a SHIMADZU/Kratos AXIS-165x. UV-Vis-NIR absorption spectra were recorded on a SHIMADZU UV-VIS-NIR SPECTROMETER UV-3150. TG-DTA data were obtained on a BRUKER TG-DTA 2000SA.

Synthesis of starch/M NPs

Water-soluble starch (1.43 g) and a metal salt (39.8 mg for $NaAuCl_4 \cdot 2H_2O$, 56.2 mg for $Na_2PtCl_6 \cdot 6H_2O$, and 17.0 mg for $AgNO_3$, respectively), and water (300 mL) were added to a 500 mL round bottom flask. The mixtures were sonicated at room temperature for 10 min and then stirred at 60 °C for 30 min to dissolve the starch. After stirring, the mixtures were cooled to 4 ºC using an ice bath. An aqueous solution of $NaBH_4$ (37.8 mg in 30 mL water) was added dropwise to the starch mixtures at 4 °C

over 10 min. The mixtures were then stirred at 4 °C for 1 h. An aqueous HCl solution (1 M, ~0.6 mL) was added to the mixtures to quench any unreacted $NaBH_4$. Anionic and cationic ion exchange resins (5 g each) (IRA-410 and IR-120B, respectively) were added to the mixtures, and stirred at room temperature for 1 h. The mixtures were then filtered to remove the resins. As a result, aqueous solutions of starch/M NPs (M = Au, Pt, and Ag) were obtained (310-320 g).

Synthesis of PAni/M NPs hybrids (M : PAni = 0.1 wt%)

PAni (emeraldine base) (500 mg) in THF (150 mL) was added to a 500 mL round bottom flask. The mixture was then sonicated at room temperature for 10 min. A previously prepared aqueous solution of starch/M NPs (M = Au, Pt, and Ag) (8.5 mL with 0.5 mg of Au, Pt, and Ag, respectively) was added dropwise to the THF solution of PAni at room temperature over 3 min. After stirring at room temperature for 17 h, the THF was removed by evaporation, and water (100 mL) was added to the mixtures. The suspensions obtained were then sonicated at room temperature for 10 min, followed by stirring at 60 °C for 30 min. The suspensions were then filtered and washed with hot water (60 °C, 100 mL x 9). The resulting residues were then dried *in vacuo*. As a result, powders of PAni/M NPs hybrids (M = Au, Pt, and Ag) were obtained (450-470 mg).

References

1. D. Saio, T. Amaya, T. Hirao, *J. Inorg. Organomet. Polym*. **2009**, *19*, 79-84.
2. E. T. Kang, K. G. Neoh, K. L. Tan, *Prog. Polym. Sci.* **1998**, *23*, 211.
3. Y. M. A. Yamada, T. Arakawa, H. Hocke, Y. Uozumi, *Angew. Chem. Int. Ed.* **2007**, *46*, 704.
4. O. P. Dimitriev and O. M. Getsko, *Synth. Met.* **1999**, *104*, 27.

Chapter 2: Synthesis of polyaniline/metal nanoparticles hybrids via template method[(2)]

Introduction

The synthesis of PAni/M NPs hybrids by the ligand exchange method is described in Chapter 1. However, using this method resulted in NPs hybrids contaminated with starch. Another synthetic method was examined, because starch residues may affect the electrical and redox properties of the PAni/M NPs hybrids.

PAni/Pd NPs hybrids have also been successfully synthesized by the template method in our laboratory.[1, 2] There is no starch contamination using this method. The template method allows for a higher loading of M NPs in the hybrids than the ligand exchange method. In my strategy, the PAni/M^{n+} complexes (M = Au, Pt, Pd, Ag, Cu, and Ni) were synthesized by mixing the PAni and metal salts in the first step. Thereafter, the PAni/M NPs hybrids (M = Au, Pt, Pd, Ag, Cu, and Ni) were synthesized by the reduction of the corresponding PAni/M^{n+} complexes in the second step (Scheme 5).

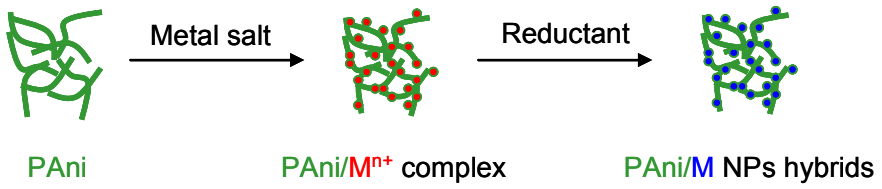

Scheme 5. Schematic drawing of the preparation of PAni/M NPs hybrids via template method.

Here, I report the synthesis of PAni/M^{n+} complexes (M = Au, Pt, Pd, Ag, Cu, and Ni), and the synthesis of PAni/M NPs hybrids (M = Au, Pt, Pd, Ag, Cu, and Ni)

through the reduction of the corresponding PAni/M^{n+} complexes.

Results and discussion

Synthesis of PAni/M^{n+} complexes

Au, Pt, Pd, Ag, Cu, and Ni were selected as metal species as they were expected to provide improved electrical and catalytic properties. PAni/M^{n+} complexes (M = Au, Pt, Pd, Ag, Cu, and Ni) were prepared as follows (Scheme 6). The metal salts listed in Table 2 were coordinated to PAni to form the corresponding PAni/M^{n+} complexes, where the ratio of the metals to PAni (w/w) were set to either 1, 5, or 10 wt% by varying the amount of metal salt added. The metal salts were dissolved in a THF/water solution that was then added dropwise to a solution of PAni (emeraldine base) in THF. The PAni/M^{n+} complexes formed spontaneously during mixing.

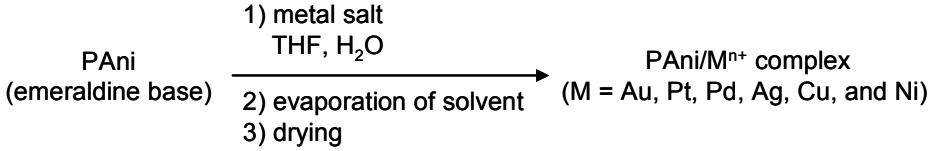

Scheme 6. The synthesis of PAni/M^{n+} (M = Au, Pt, Pd, Ag, Cu, and Ni) complexes.

Table 2. The used metal salts in synthesis of PAni/M^{n+} complexes.

Metals	M^{n+}
Au	$NaAuCl_4 \cdot 2H_2O$
Pt	$Na_2PtCl_6 \cdot 6H_2O$
Pd	$Pd(OAc)_2$
Ag	$AgNO_3$
Cu	CuCl
Ni	$NiCl_2$

All of the solutions of PAni/M^{n+} complexes were a dark violet color. Figure 11 shows a selected region of FT-IR spectra of PAni and PAni/M^{n+} complexes (M = Au, Pt, Pd, Ag, Cu, and Ni, 10 wt%). All of the spectra were similar. Peaks at approximately 1600 and 1500 cm^{-1}, which are attributable to the quinonediimine and the phenylenediamine moieties of PAni, respectively,[3] were observed. The peak intensity ratio (quinonediimine/phenylenediamine) provided a qualitative measure of their mole ratio.[4] The wavenumber of the peaks and the intensity ratios of quinonediimine/phenylenediamine for each PAni/M^{n+} hybrid are summarized in Table 3. The ratio of quinonediimine/phenylenediamine for PAni was approximately 0.4 : 0.6, which was estimated by the literature method.[4] The peak intensity ratio of quinonediimine/phenylenediamine for all of the PAni/M^{n+} complexes increased when compared to PAni. The peak intensity ratio of quinonediimine/phenylenediamine also increased with higher metal content. This indicated the partial oxidation of the main chain structure of PAni. This oxidation was catalyzed by M^{n+} under air (molecular oxygen). It is also possible that the PAni used was slightly rich in the reduced form (0.56, intensity ratio of quinonediimine/phenylenediamine), and therefore it might be partially oxidized easily. For PAni/Cu^{+} complexes, the oxidation power was lower than that of the other PAni/M^{n+} complexes. A reason for this phenomenon is that oxygen in air could oxidize Cu^{+} to Cu^{2+} species.

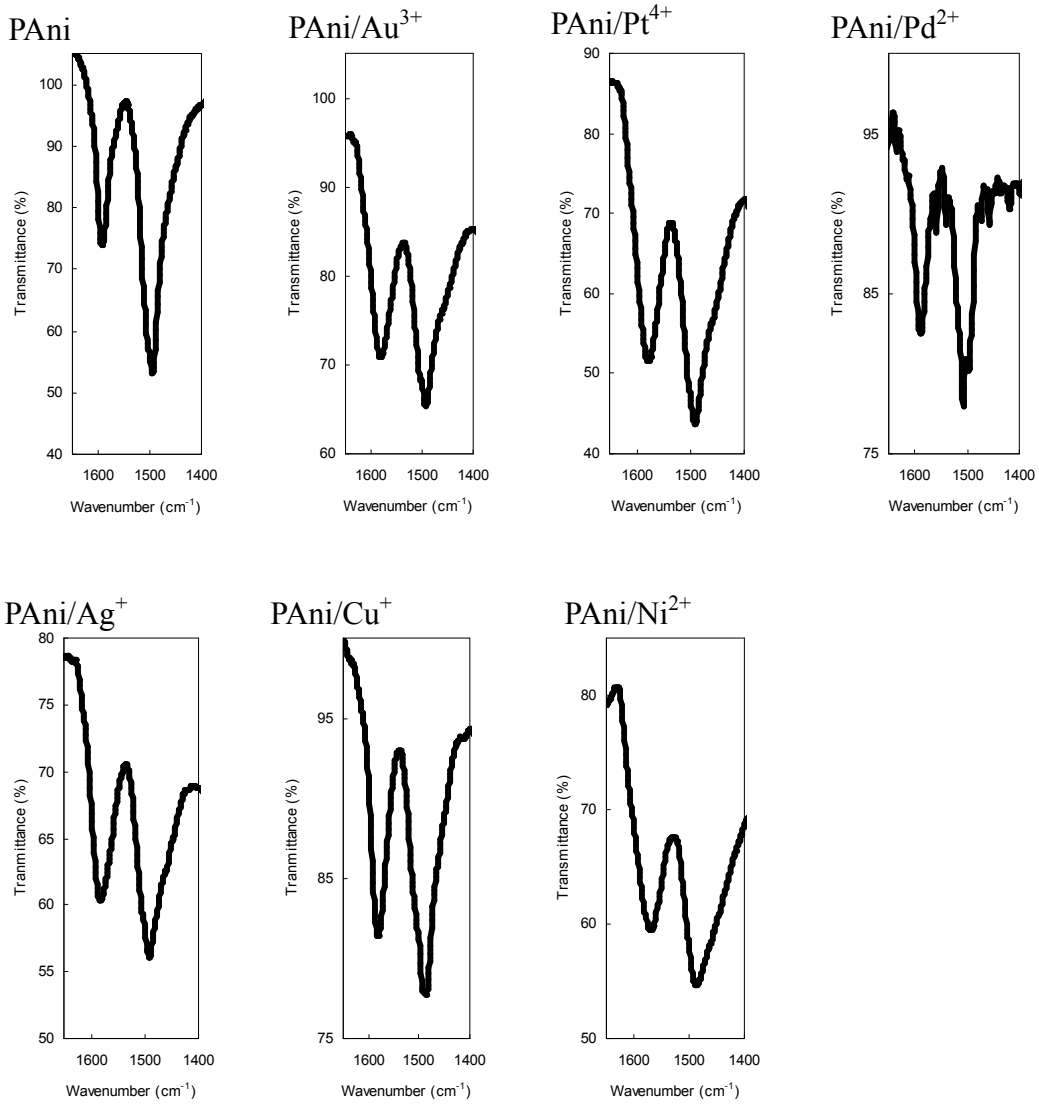

Figure 11. Selected region of the FT-IR spectra of PAni and PAni/ M^{n+} complexes (M = Au, Pt, Pd, Ag, Cu, and Ni, 10 wt%).

Table 3. Wavenumber (cm^{-1}) and transmittance (%) of the peaks at approximately 1600 and 1500 cm^{-1} in the IR (ATR) spectra of PAni and PAni/ M^{n+} complexes (M = Au, Pt, Pd, Ag, Cu, and Ni, 10 wt%), and the peak intensity ratio of quinonediimine/phenylenediamine.

	Wt %	Peak around 1600 cm^{-1} (quinoiddiimine)		Peak around 1500 cm^{-1} (phenylenediamine)		Peak intensity ratio of quinoidediimine/ phenylenediamine[a]
		Waven umber (cm^{-1})	Transmit tance (%)	Waven umber (cm^{-1})	Transmit tance (%)	
PAni		1593	74	1495	53	0.55
$PAni/Au^{3+}$	1	1592	76	1494	64	0.67
	5	1584	67	1492	58	0.79
	10	1581	71	1493	65	0.83
$PAni/Pt^{4+}$	1	1591	85	1495	76	0.63
	5	1585	68	1493	58	0.76
	10	1578	52	1492	44	0.86
$PAni/Pd^{2+}$	1	1588	72	1496	67	0.85
	5	1589	85	1492	80	0.75
	10	1589	82	1507	78	0.82
$PAni/Ag^{+}$	1	1589	65	1493	57	0.81
	5	1586	68	1493	63	0.86
	10	1583	60	1492	56	0.91
$PAni/Cu^{+}$	1	1588	83	1494	77	0.74
	5	1585	91	1494	88	0.75
	10	1581	81	1488	78	0.86
$PAni/Ni^{2+}$	1	1588	59	1493	44	0.73
	5	1579	83	1492	79	0.81
	10	1569	60	1487	55	0.89

[a](100-[Transmittance of quinonediimine])/(100-[Transmittance of phenylenediamine])

Synthesis of PAni/M NPs hybrids

PAni/M NPs hybrids (M = Au, Pt, Pd, Ag, Cu, and Ni) were synthesized by the reduction of the corresponding PAni/M^{n+} complexes (Scheme 7). An aqueous solution of $NaBH_4$ was added dropwise to the PAni/M^{n+} complexes (M = Au, Pt, Pd, Ag, Cu, and

Ni). After the reaction, the mixture was washed with water to remove residual $NaBH_4$ and its derivatives. 400-500 mg of PAni/M NPs hybrids (M = Au, Pt, Pd, Ag, Cu, and Ni) were obtained starting from 500 mg of PAni.

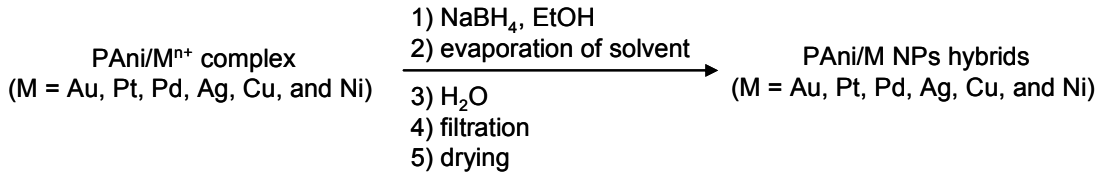

Scheme 7. The synthesis of PAni/M NPs hybrids.

Figure 12 shows a selected region of the FT-IR spectra of PAni and PAni/M NPs hybrids (M = Au, Pt, Pd, Ag, Cu, and Ni, 10 wt%). All of the spectra were similar. The peaks at approximately 1600 and 1500 cm^{-1}, which were attributable to the quinonediimine and the phenylenediamine of PAni respectively,[3] were observed. The peak intensity ratio of quinonediimine/phenylenediamine were lower for all of PAni/M NPs hybrids (M = Au, Pt, Pd, Ag, Cu, and Ni) when compared to those of the corresponding PAni/M^{n+} complexes (M = Au, Pt, Pd, Ag, Cu, and Ni) as summarized in Table 4. This phenomenon was caused by the partial reduction of the PAni main chain structure by $NaBH_4$.

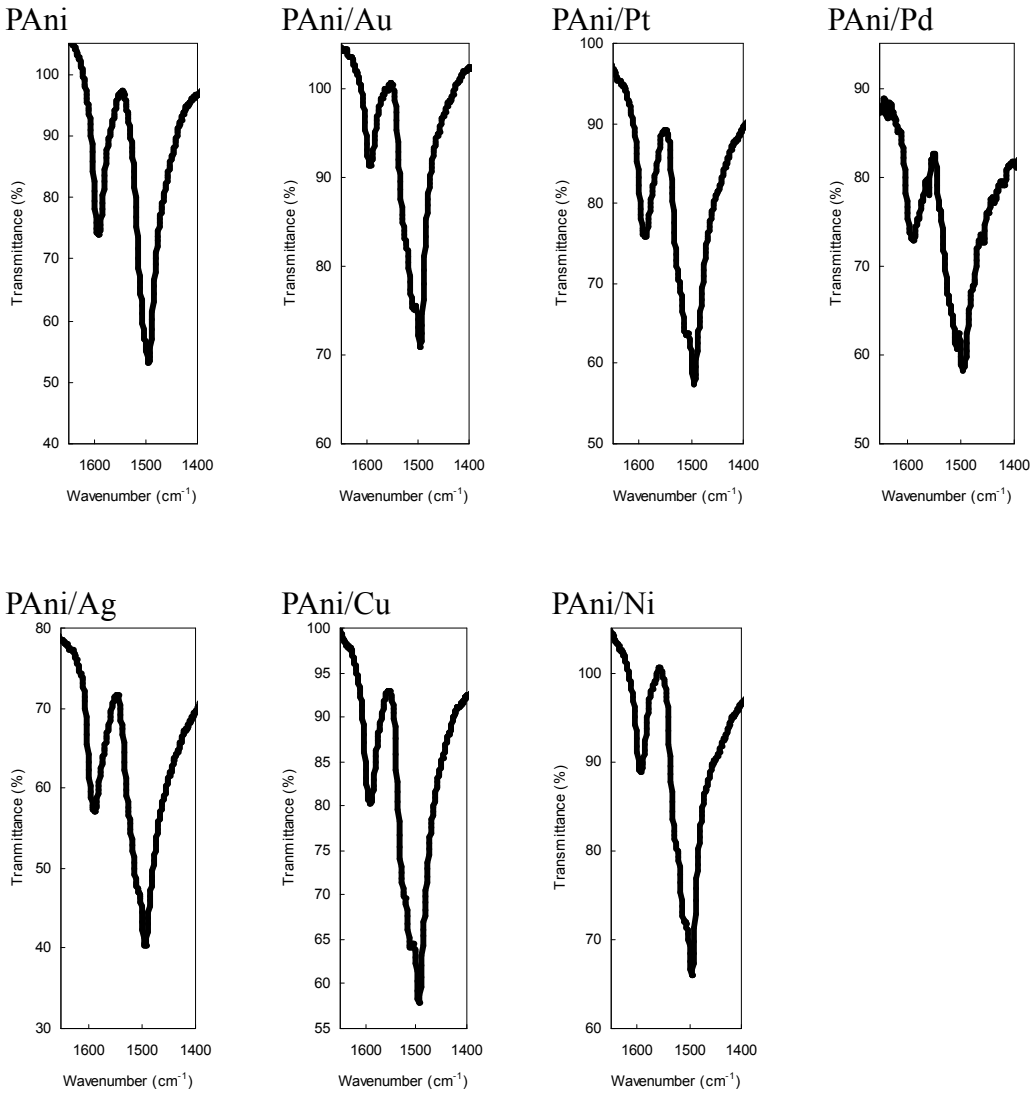

Figure 12. Selected region of the FT-IR spectra of PAni and PAni/M NPs hybrids (M = Au, Pt, Pd, Ag, Cu, and Ni, 10 wt%).

Table 4. Wavenumber (cm^{-1}) and transmittance (%) of the peaks at approximately 1600 and 1500 cm^{-1} in the IR (ATR) spectra of PAni and PAni/M NPs hybrids (M = Au, Pt, Pd, Ag, Cu, and Ni, 10 wt%), and the peak intensity ratio of quinonediimine/phenylenediamine.

	Wt %	Peak around 1600 cm^{-1} (quinoiddiimine)		Peak around 1500 cm^{-1} (phenylenediamine)		Peak intensity ratio of quinoidediimine/ phenylenediamine[a]
		Waven umber (cm^{-1})	Transmit tance (%)	Waven umber (cm^{-1})	Transmit tance (%)	
PAni		1593	74	1495	53	0.55
PAni/Au	1	1593	90	1495	74	0.38
	5	1594	85	1496	60	0.38
	10	1594	91	1496	71	0.31
PAni/Pt	1	1594	82	1495	64	0.50
	5	1592	89	1496	78	0.50
	10	1588	76	1495	57	0.56
PAni/Pd	1	1593	86	1507	77	0.61
	5	1588	76	1496	69	0.77
	10	1589	73	1496	58	0.64
PAni/Ag	1	1593	72	1495	49	0.55
	5	1593	61	1495	33	0.58
	10	1588	57	1494	40	0.72
PAni/Cu	1	1592	96	1495	82	0.22
	5	1590	73	1495	48	0.52
	10	1591	80	1496	58	0.48
PAni/Ni	1	1596	87	1495	56	0.30
	5	1594	79	1495	50	0.42
	10	1594	89	1496	66	0.32

[a](100-[Transmittance of quinonediimine])/(100-[Transmittance of phenylenediamine])

Figure 13 shows the UV-Vis-NIR absorption spectra of PAni and PAni/M NPs hybrids (M = Au, Pt, Pd, Ag, Cu, and Ni, 10 wt%). The characteristic peaks around 330 and 600 nm, which are attributable to the π-π* transition of the phenyl ring and the charge transfer (CT) from the benzenoid to the quinoid, respectively,[5] were observed.

The wavelength (nm) and absorbance (%) for the peak at approximately 600 nm in these spectra are summarized in Table 5. These are typical spectra for the emeraldine base of PAni. Decreased absorbance was observed for all PAni/M NPs hybrids relative to PAni. This hypochromic effect was derived from intermolecular aggregation and/or intramolecular conformational changes that might be induced by the presence of M NPs. A hypochromic effect on the emeraldine base of PAni that was induced by the solvent has been observed and discussed in the literature.[6] For PAni/Cu NPs hybrid, a blue shift of the CT band was observed. According to our previous work,[7] the complexation of PAni with Cu^{2+} induced a similar blue shift. The blue shift observed could indicate the presence of Cu^{2+}, which might have been unreacted in the synthesis or formed later via a redox reaction between Cu^{0} and PAni or oxidized under air (molecular oxygen).

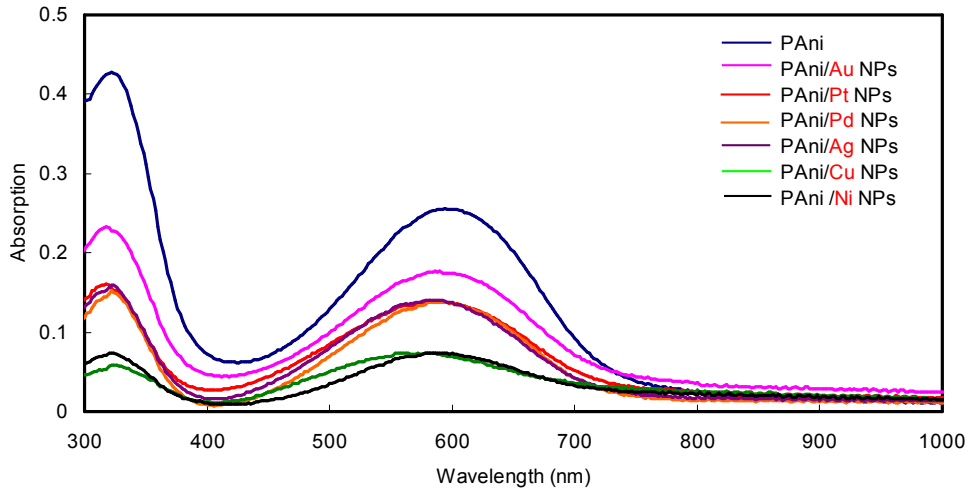

Fig. 13. UV-Vis-NIR absorption spectra ($1.0x10^{-4}$ M based on aniline unit, NMP) of PAni and PAni/M NPs hybrids (M = Au, Pt, Pd, Ag, Cu, and Ni, 10 wt%).

Table 5. Wavelength (nm) and absorbance (%) for the peak around 600 nm in UV-Vis-NIR absorption spectra of PAni and PAni/M NPs hybrids (M = Au, Pt, Pd, Ag, Cu, and Ni, 10 wt%) ($1.0x10^{-4}$ M based on aniline unit, NMP).

	Peak around 600 nm	
	Wavelength (nm)	Absorbance (%)
PAni	594	0.26
PAni/Au	588	0.18
PAni/Pt	582	0.14
PAni/Pd	590	0.14
PAni/Ag	584	0.14
PAni/Cu	560	0.073
PAni/Ni	586	0.074

Figure 14 shows the TEM images of PAni/M NPs hybrids (M = Au, Pt, Pd, Ag, Cu, and Ni, 10 wt%). PAni/Au, Pt, and Pd NPs hybrids (5 wt%) have M NPs (mainly in the range of 2-3 nm). However, M NPs were not clearly observed in PAni/Ag, Cu, and Ni NPs hybrids (5 wt%). The SEM-EDX images of PAni/M NPs hybrids (M = Au, Pt, Pd, Ag, Cu, and Ni, 10 wt%) (Figure 15), showed a uniform dispersion of the metals. Some M NPs could have been formed before the treatment with $NaBH_4$. According to the literature, $NaBH_4$ can reduce Ag^{+},[8] Ni^{2+},[9] and Cu^{2+} [10] to form the corresponding M NPs. Therefore, M^{n+} was expected to be reduced in these experiments. Formation of smaller (subnano) particles could be a reason why NPs were not observed in the TEM images of PAni/Ag, Cu, and Ni NPs hybrids (5 wt%).

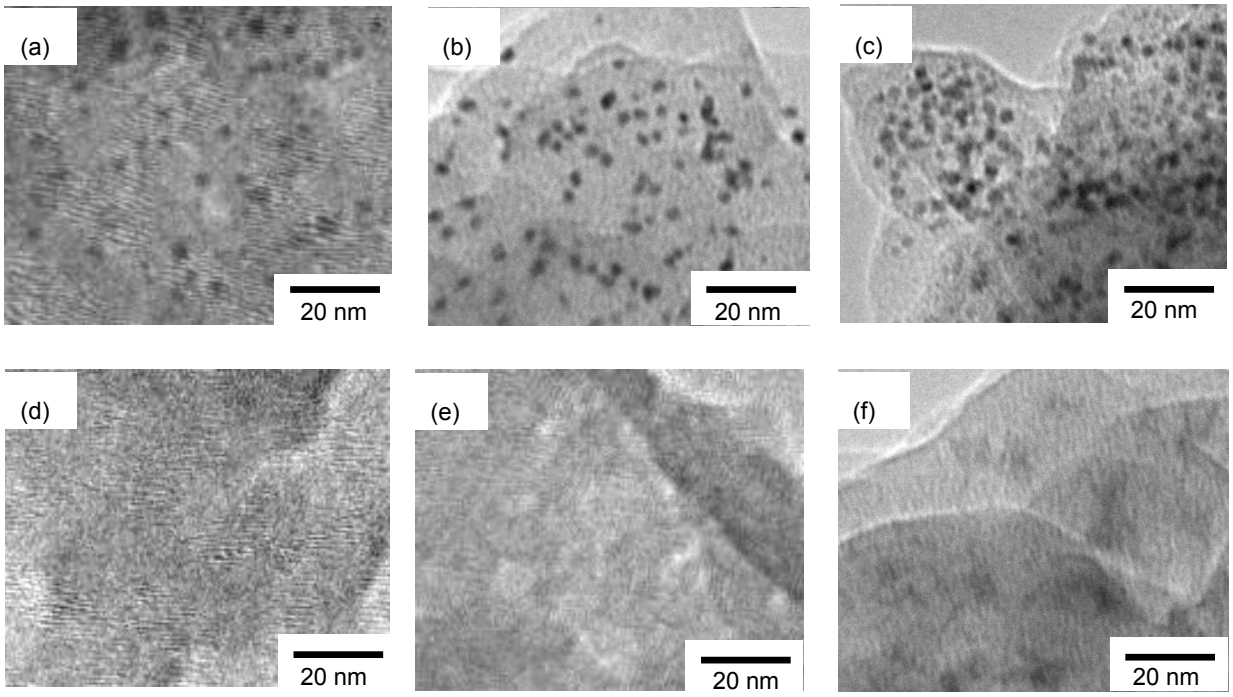

Figure 14. TEM images of (a) PAni/Au NPs hybrids (5 wt%), (b) PAni/Pt NPs hybrids (5 wt%), (c) PAni/Pd NPs hybrids (5 wt%), (d) PAni/Ag NPs hybrids (5 wt%), (e) PAni/Cu NPs hybrids (5 wt%), and (f) PAni/Ni NPs hybrids (5 wt%).

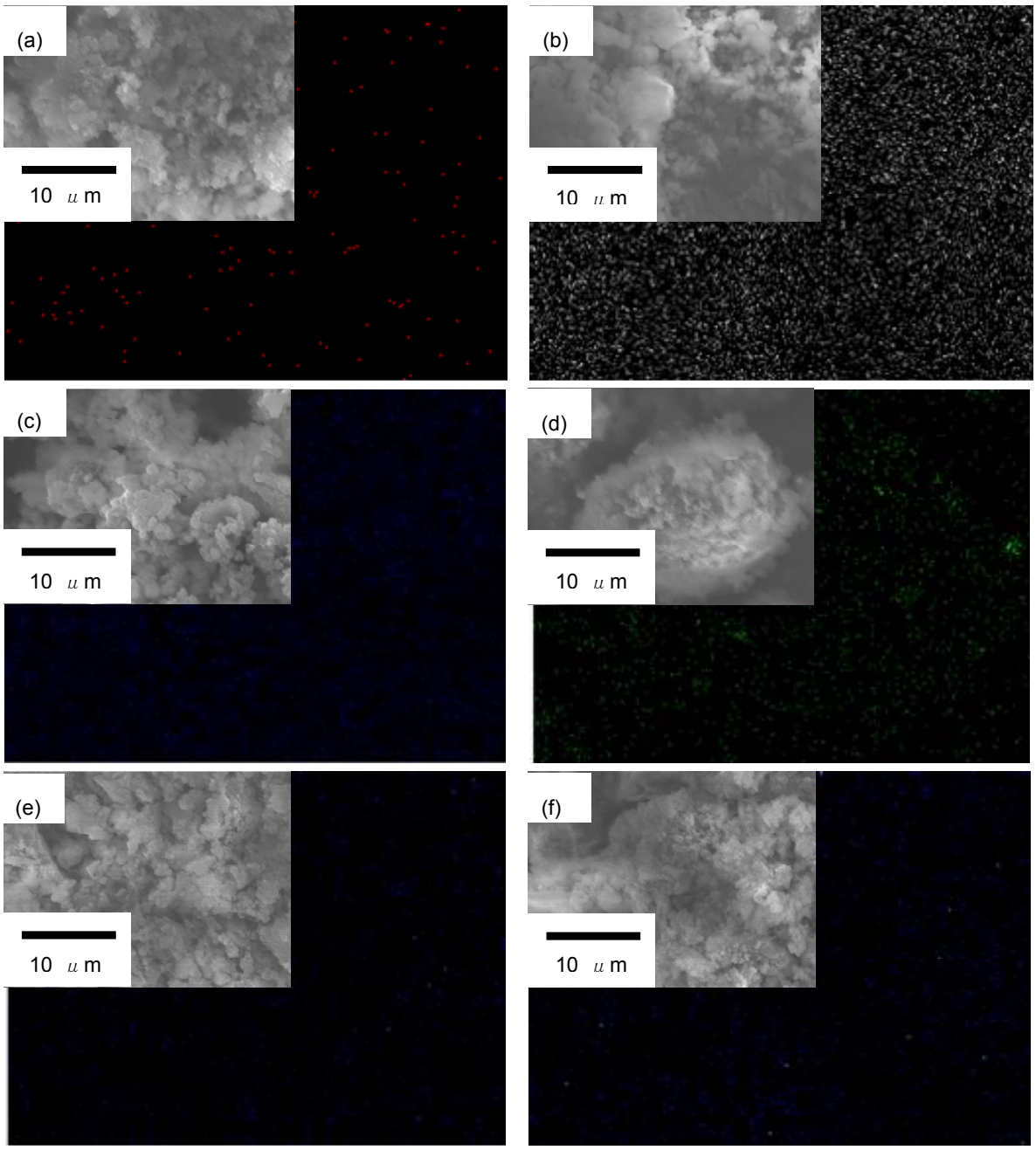

Figure 15. SEM-EDX images of (a) PAni/Au NPs hybrids (5 wt%), (b) PAni/Pt NPs hybrids (5 wt%), (c) PAni/Pd NPs hybrids (5 wt%), (d) PAni/Ag NPs hybrids (5 wt%), (e) PAni/Cu NPs hybrids (5 wt%), and (f) PAni/Ni NPs hybrids (5 wt%).

Conclusion

PAni/M NPs hybrids (M = Au, Pt, Pd, Ag, Cu, and Ni) were produced via our template method. The IR spectra suggest that partial oxidation of the main chain structure of PAni occurred in the complexation step. Also, partial reduction of the main chain structure of PAni occurred during the reduction of the complexes. In the UV-Vis-NIR absorption spectra of PAni/M NPs hybrids (M = Au, Pt, Pd, Ag, Cu, and Ni), a hypochromic effect in the π-π* and CT bands was observed. M NPs (mainly in the range of 2-3 nm) were observed in PAni/Au, Pt, and Pd NPs hybrids, but not for PAni/Ag, Cu, and Ni NPs hybrids. However, the SEM-EDX images of the PAni/M NPs hybrids (M = Au, Pt, Pd, Ag, Cu, and Ni) showed a uniform dispersion of the metals.

Experimental section

Instrumentation and chemicals

All reagents were purchased from commercial sources and used without further purification. PAni (emeraldine base, M_W: *ca.* 10000) was purchased from Aldrich. $NaAuCl_4 \cdot 2H_2O$, $Na_2PtCl_6 \cdot 6H_2O$, $Pd(OAc)_2$, CuCl, and $NiCl_2$ were purchased from Kanto Chemical. $AgNO_3$ was purchased from Wako Pure Chemical Industries. The Elemental Analysis Section of Osaka University performed the elemental analysis. FT-IR spectra were recorded using the ATR technique with a JASCO FT/IR-4200 spectrometer. UV-Vis-NIR absorption spectra were recorded on a SHIMADZU UV-VIS-NIR SPECTROMETER UV-3150. TEM images were recorded on a JEOL JEM-1010. SEM-EDX images were recorded on a Hitachi S4300 (SEM) and Horiba EMAX (EDX).

Synthesis of PAni/M^{n+} complexes

Polyaniline (500 mg) and THF (150 mL) were added to a 500 mL round bottom flask. The mixtures were sonicated at room temperature to dissolve the PAni. Solutions of M^{n+} (Table 6) in THF (25 mL) {for $AgNO_3$, CuCl, and $NiCl_2$, THF/H_2O (20 mL/5 mL, 20 mL/10 mL, 20 mL/5 mL, respectively) was used due to the low solubility of M^{n+}} were added dropwise to the stirred solution of PAni at room temperature over 30 min. To form a suspension of PAni/M^{n+} complexes, the reaction mixtures were stirred at room temperature for ~1 h. The solvent was then removed by evaporation and the wet powders obtained were dried *in vacuo* to yield PANI/M^{n+} complexes. The results of the elemental analysis (for H, C, and N) of PANI/M^{n+} complexes are summarized in Table 7.

Table 6. The used metal salts in synthesis of PAni/M^{n+} complexes.

Metal amount to PAni	1 wt%		5 wt%		10 wt%	
M^{n+}	Amount (mg)	Mole (mmol)	Amount (mg)	Mole (mmol)	Amount (mg)	Mole (mmol)
$NaAuCl_4 \cdot 2H_2O$	10.1	0.025	50.5	0.127	101.0	0.254
$Na_2PtCl_6 \cdot 6H_2O$	14.4	0.026	72.0	0.128	144.0	0.256
$Pd(OAc)_2$	10.5	0.047	52.7	0.235	105.5	0.470
$AgNO_3$	7.9	0.046	39.4	0.232	78.7	0.464
CuCl	7.8	0.079	38.9	0.393	77.9	0.787
$NiCl_2$	11.0	0.085	55.2	0.426	110.4	0.852

Table 7. Elemental analysis of PAni/M^{n+} complexes.

	Wt %	Calcd			Found		
		H	C	N	H	C	N
PAni/Au^{3+}	1	5.22[a]	74.34[a]	14.45[a]	5.31	74.45	13.60
	5	4.92[a]	69.12[a]	13.43[a]	4.87	69.35	13.02
	10	4.61[a]	63.54[a]	12.35[a]	4.48	63.54	11.99
PAni/Pt^{4+}	1	5.21[a]	73.75[a]	14.33[a]	5.24	74.18	13.83
	5	4.79[b]	68.05[b]	13.23[b]	4.78	67.57	12.74
	10	4.50[b]	60.58[b]	11.78[b]	4.44	60.53	11.41
PAni/Pd^{2+}	1	-	-	-	Not Measured	Not Measured	Not Measured
	5	4.79	73.99	13.98	5.25	74.17	13.37
	10	5.10[c]	64.14[c]	11.80[c]	4.69	64.54	11.83
PAni/Ag^{+}	1	5.22[a]	74.65[a]	14.63[a]	5.26	73.97	13.64
	5	5.06[d]	68.96[d]	13.97[d]	4.95	68.79	13.41
	10	4.82[e]	63.79[e]	13.44[e]	4.64	63.72	12.91
PAni/Cu^{+}	1	5.36[d]	72.96[d]	14.18[d]	5.05	73.29	13.90
	5	5.07[d]	69.02[d]	13.41[d]	4.67	68.88	13.19
	10	4.87	63.36	12.32	4.29	62.84	12.02
PAni/Ni^{2+}	1	-	-	-	Not Measured	Not Measured	Not Measured
	5	5.06[c]	65.74[c]	12.78[c]	4.97	65.39	12.52
	10	5.09[a]	56.03[a]	10.89[a]	4.61	55.77	10.72

[a] 0.25 equiv of H_2O (based on the aniline unit) was added to the calculated value.

[b] 0.125 equiv of H_2O (based on the aniline unit) was added to the calculated value.

[c] 0.5 equiv of H_2O (based on the aniline unit) was added to the calculated value.

[d] 0.375 equiv of H_2O (based on the aniline unit) was added to the calculated value.

[e] 0.45 equiv of H_2O (based on the aniline unit) was added to the calculated value.

Synthesis of PAni/M NPs hybrids

A solution of $NaBH_4$ (10 equiv. relative to the M^{n+}) in ethanol (25 mL) was added dropwise to a suspension of PAni/M^{n+} complex in THF over 30 min to prepare PAni/M NPs hybrids (M = Au, Pt, Pd, Ag, Cu, and Ni). The mixtures were stirred at

room temperature for 1 h (for CuCl and $NiCl_2$, the mixtures were stirred at 60 °C for 3 h). The solvent was removed by evaporation and water (100 mL) was added. The resulting suspension was sonicated for 10 min. at room temperature. The suspension was filtered, and the residue was dried *in vacuo*. 400-500 mg of PAni/M NPs hybrids was obtained from 500 mg of PAni. The results of elemental analysis (for H, C, and N) for the PAni/M NPs hybrids are summarized in Table 8.

Table 8. Elemental analysis of PAni/M NPs hybrids.

	Wt %	Calcd			Found		
		H	C	N	H	C	N
PAni/Au	1	5.25[a]	75.05[a]	14.59[a]	5.37	76.34	14.55
	5	5.05[a]	72.32[a]	14.06[a]	5.09	73.19	14.06
	10	4.84[a]	69.18[a]	13.45[a]	4.90	70.18	13.37
PAni/Pt	1	5.11[b]	76.86[b]	14.94[b]	5.29	76.43	14.67
	5	4.92[b]	74.00[b]	14.38[b]	5.00	74.14	14.21
	10	4.84[b]	69.18[b]	13.45[b]	4.80	69.55	13.36
PAni/Pd	1	5.25[a]	75.06[a]	14.59[a]	5.17	75.38	14.54
	5	5.06[a]	72.33[a]	14.06[a]	4.91	72.00	13.97
	10	4.83[a]	69.18[a]	13.45[a]	4.69	68.25	13.30
PAni/Ag	1	5.25[a]	75.05[a]	14.59[a]	5.33	76.07	14.63
	5	5.06[a]	72.32[a]	14.06[a]	5.11	72.87	14.00
	10	4.84[a]	69.18[a]	13.45[a]	4.78	69.33	13.25
PAni/Cu	1	5.25[a]	75.05[a]	14.59[a]	5.22	75.57	14.50
	5	4.92[b]	64.00[b]	14.38[b]	5.12	73.41	14.06
	10	4.97[d]	67.71[d]	13.16[d]	4.95	67.46	12.54
PAni/Ni	1	5.25[a]	75.06[a]	14.59[a]	5.38	75.20	14.42
	5	5.32[c]	69.20[c]	13.45[c]	5.21	68.75	13.05
	10	5.57[f]	61.24[f]	11.90[f]	4.79	61.86	11.87

[a] 0.25 equiv of H_2O (based on the aniline unit) was added to the calculated value.

[b] 0.125 equiv of H_2O (based on the aniline unit) was added to the calculated value.

[c] 0.5 equiv of H_2O (based on the aniline unit) was added to the calculated value.

[d] 0.375 equiv of H_2O (based on the aniline unit) was added to the calculated value.

[e] 0.45 equiv of H_2O (based on the aniline unit) was added to the calculated value.

[f] 1 equiv of H_2O (based on the aniline unit) was added to the calculated value.

References

1. T. Amaya, D. Saio, T. Hirao, *Macromol. Symp.* **2008**, *270*, 88-94.
2. T. Amaya, D. Saio, T. Hirao, *Tetrahedron Lett.* **2007**, *48*, 2729-2732.
3. E. T. Kang, K. G. Neoh, K. L. Tan, *Prog. Polym. Sci.* **1998**, *23*, 211.
4. G. E. Asturias, A. G. MacDiarmid, R. P. Mccall, A. *J. Epstein, Synth. Met.* **1989**, *29*, E157.
5. L. L. Premvardhan, S. Wachsmann-Hogiu, L. A. Peteanu, D. J. Yaron, P.-C. Wang, W. Wang, A. G. MacDiarmid, *J. Chem. Phys.* **2001**, *115*, 4359.
6. O. P. Dimitriev and O. M. Getsko, *Synth. Met.* **1999**, *104*, 27.
7. M. Higuchi, D. Imoda, T. Hirao, *Macromolecules* **1996**, *29*, 8277.
8. G. Chang, Y. Lio, W. Lu, X. Qin, A.M. Asiri, A.O. AI-Youbi, X. Sun, *Catal. Sci. Tecnol.* **2012**, *2*, 800.
9. K. Nouneh, M. Oyama, R. Diaz, M. Abd-Lefdil, I. V. Kityk, M. Bousmina, *J. Alloys Compd.* **2011**, *509*, 5882.
10. S. Sharma, C. Nirkhe, S. Pethkar, A. A. Athawale, *Sens. Actuators B*, **2002**, *85*, 131.

Chapter 3: Conductivity and catalytic properties for active oxygen generation of polyaniline/metal nanoparticles hybrids[(2), (3)]

Introduction

The electrical and redox properties were investigated for the PAni/M NPs hybrids and PAni/M^{n+} complexes (M = Au, Pt, Pd, Ag, Cu, and Ni, 10 wt%) produced in Chapter 2. Though there is existing literature on the synthesis and evaluation of PAni/M NPs hybrids, there are few reports evaluating those synthesized by this or a similar method.[1-29] This study was focused on investigating the effect of the hybridized metal species. Conductivity and active oxygen generation were selected to evaluate the electrical and redox properties, respectively. These evaluations were carried out after proton doping of the PAni/M NPs hybrids and the PAni/M^{n+} complexes (M = Au, Pt, Pd, Ag, Cu, and Ni, 10 wt%).

Here, I report the proton doping of PAni/M NPs hybrids and PAni/M^{n+} complexes (M = Au, Pt, Pd, Ag, Cu, and Ni, 10 wt%), and the evaluation of the conductivity of, and generation of active oxygen in water by, H^+-PAni/M NPs hybrids (M = Au, Pt, Pd, Ag, Cu, and Ni).

Results and discussion

Proton doping

The proton doping was performed as follows (Scheme 8). PAni or the PAni/M NPs hybrids or the PAni/M^{n+} complexes (M = Au, Pt, Pd, Ag, Cu, and Ni, 10 wt%) were dissolved in *N*-methyl-2-pyrrolidone (NMP). *p*-Toluenesulfonic acid (*p*-TsOH)

was then added as a dopant. Upon addition of the acid, the color of the solutions changed from purple to green, which is the characteristic color of the emeraldine salt. After doping, the solvent was removed by evaporation and dried *in vacuo* to yield H^+-PAni/M NPs hybrids and H^+-PAni/M^{n+} complexes (M = Au, Pt, Pd, Ag, Cu, and Ni, 10 wt%).

(a)

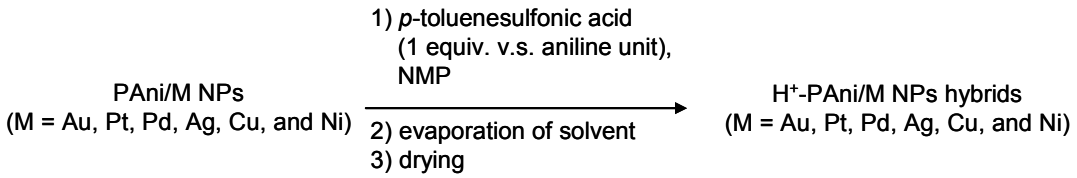

(b)

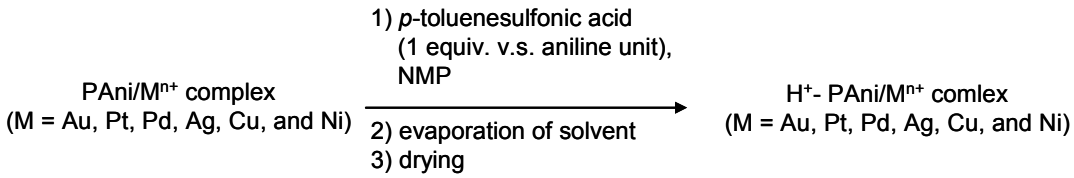

Scheme 8. Proton doping of (a) PAni/M NPs hybrids and (b) PAni/M^{n+} complexes (M = Au, Pt, Pd, Ag, Cu, and Ni, 10 wt%).

Figure 16 shows the UV-Vis-NIR absorption spectra of H^+-PAni/M NPs hybrids (M = Au, Pt, Pd, Ag, Cu, and Ni, 10 wt%). The characteristic peaks at approximately 330 and 600 nm, which are attributable to the π-π* transition of the phenyl ring and the charge transfer (CT) from the benzenoid to the quinoid, respectively,[30] were observed. For H^+-PAni, H^+-PAni/Au and Ni NPs hybrids, a peak

around 460 nm, which is attributable to a polaron band,[30] was observed. However, for H^+-PAni/Pt, Pd, Ag, and Cu NPs hybrids, the absorbance of the polaron band was not observed and it suggested that the doping was inefficient. For H^+-PAni/Cu NPs hybrid, a blue shift of the CT band was observed. According to our previous work,[31] the complexation of PAni with Cu^{2+} induce the similar blue shift. The blue shift observed could indicate the presence of Cu^{2+}, which might have been unreacted in the synthesis or formed later via a redox reaction between Cu^0 and PAni.

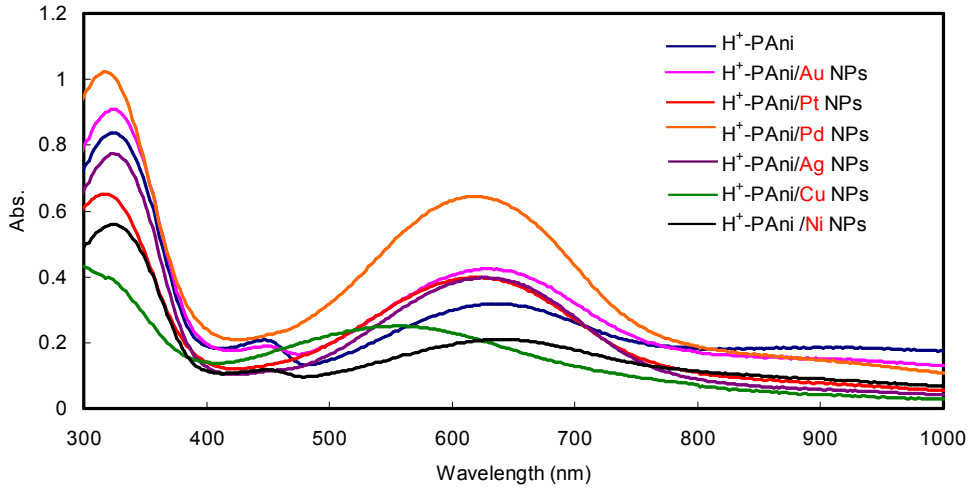

Figure 16. UV-Vis-NIR absorption spectra ($1.0x10^{-4}$ M based on the aniline unit, NMP) of H^+-PAni and H^+-PAni/M NPs hybrids (M = Au, Pt, Pd, Ag, Cu, and Ni, 10 wt%).

Figure 17 shows the UV-Vis-NIR absorption spectra of the H^+-PAni/M^{n+} complexes (M = Au, Pt, Pd, Ag, Cu, and Ni, 10 wt%). The characteristic peaks at approximately 330 and 600 nm, which are attributable to the π-π* transition of the phenyl ring and the charge transfer (CT) from the benzenoid to the quinoid, respectively,[30] were observed. For H^+-PAni, a peak at approximately 460 nm,

attributable to a polaron band,[30] was observed. However, for H^+-PAni/M^{n+} complexes (M = Au, Pt, Pd, Ag, Cu, and Ni, 10 wt%), the absorbance of the polaron band was not observed and this suggested that doping was inefficient. For the H^+-PAni/Cu^+ complex, a blue shift of the CT band was observed. According to our previous work,[31] the complexation of PAni with Cu^{2+} induces a similar blue shift. For H^+-PAni/Pd^{2+}complex, the characteristic peaks in PAni were not observed. This could be the result of oxidation of the main chain of PAni, but the details are not clear yet.

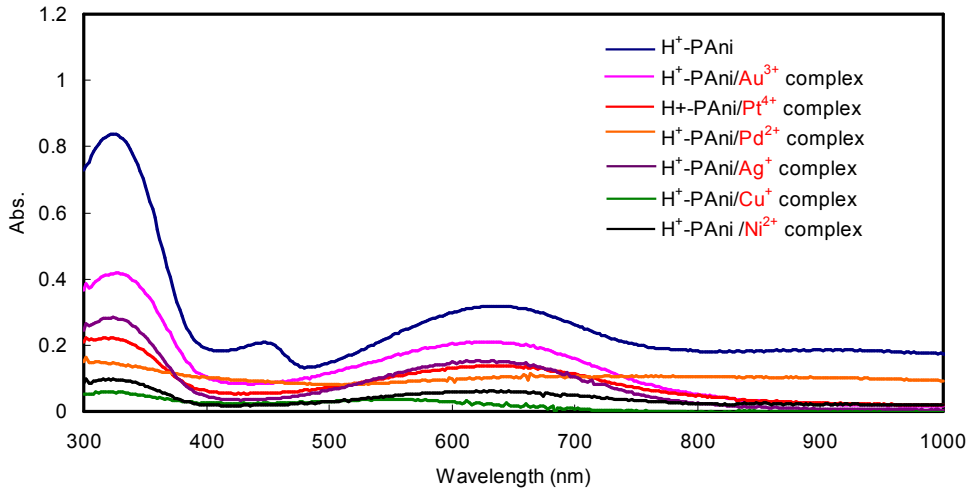

Figure 17. UV-Vis-NIR absorption spectra ($1.0x10^{-4}$ M based on the aniline unit, NMP) of H^+-PAni and H^+-PAni/M^{n+} complexes (M = Au, Pt, Pd, Ag, Cu, and Ni, 10 wt%).

Measurement of conductivity

The conductivity of the H^+-PAni/M NPs hybrids and H^+-PAni/M^{n+} complexes (M = Au, Pt, Pd, Ag, Cu, and Ni) were measured via the volume specific resistance of a pressed pellet (Table 9 and 10).

The conductivity of H^+-PAni was 2 x 10^{-5} S/cm. For H^+-PAni/Au, Pt, Pd, Ag,

and Cu NPs hybrids, the conductivity was one or two orders of magnitude lower than in H^+-PAni. In Chapter 2, the partial reduction of PAni in the IR spectra of the PAni/M NPs hybrids was observed. The reduction of PAni may be a reason why the conductivity decreased. However, for H^+-PAni/Ni NPs hybrid, the conductivity was two orders of magnitude higher than in H^+-PAni.

For H^+-PAni/M^{n+} complexes (M = Au, Pt, Pd, Ag, Cu, and Ni), the conductivity was lower than in H^+-PAni. In Chapter 2, the partial oxidation of PAni in the IR spectra of the PAni/M^{n+} complexes was observed. The oxidation of PAni is considered to be one of the reasons for the decreased conductivity. Inefficient doping may also be a reason for lower conductivity as well. The doping of PAni could have been hindered by the coordination of metal to the quinonediimine.

Table 9. Conductivity of H^+-PAni/M NPs hybrids (M = Au, Pt, Pd, Ag, Cu, and Ni).

	Conductivity (S/cm)
H^+-PAni	2×10^{-5}
H^+-PAni/Au NPs	2×10^{-7}
H^+-PAni/Pt NPs	3×10^{-6}
H^+-PAni/Pd NPs	5×10^{-6}
H^+-PAni/Ag NPs	3×10^{-7}
H^+-PAni/Cu NPs	1×10^{-6}
H^+-PAni/Ni NPs	3×10^{-3}

Table 10. Conductivity of H^+-PAni/M^{n+} complexes

(M = Au, Pt, Pd, Ag, Cu, and Ni).

	Conductivity (S/cm)
H^+-PAni	2×10^{-5}
H^+-PAni/Au^{3+} complex	3×10^{-5}
H^+-PAni/Pt^{4+} complex	9×10^{-7}
H^+-PAni/Pd^{2+} complex	7×10^{-7}
H^+-PAni/Ag^+ complex	4×10^{-5}
H^+-PAni/Cu^+ complex	N/A
H^+-PAni/Ni^{2+} complex	4×10^{-7}

Preparation of electrode

UV-curable dipentaerythritol hexaacrylate (DPHA) was used as a binder. A coating fluid was prepared by adding a solution of DPHA to the stirred solution of H^+-PAni/M NPs hybrids (M = Au, Pt, Pd, Ag, Cu, and Ni) in NMP. A film was formed by spin coating of the fluid onto an ITO electrode, which was then cured with UV irradiation. The thicknesses of the films obtained were 190-230 nm. Figure 18 shows the UV-Vis-NIR absorption spectra of each electrode film. The characteristic peaks around 330 and 450-500 nm, which are attributable to the π-π^* transition of the phenyl ring and a polaron band,[30] were observed.

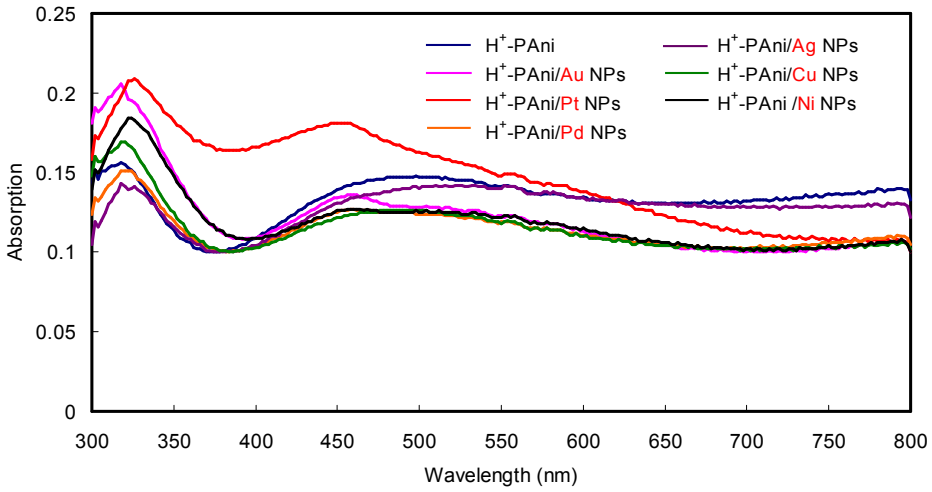

Figure 18. UV-Vis-NIR absorption spectra of the electrode films.

Hydrogen peroxide generation

Hydrogen peroxide was quantified instead of the superoxide radical anion because the superoxide radical anion disproportionates to hydrogen peroxide and oxygen.[32] Table 11 shows the concentration of hydrogen peroxide generated by each electrode in physiological saline. First, the generation of hydrogen peroxide by the H^+-PAni electrode was examined. The concentration of hydrogen peroxide in the physiological saline (50 mL) was 2.0 ppm after applying a voltage (2.5 V) for 6 h. This experiment was repeated five times to investigate the repetition durability of the electrode. The concentration of hydrogen peroxide decreased gradually and became 0 ppm after the fifth cycle. The color of the electrode film also changed from green to purple. For the H^+-PAni/Au, Pt, and Pd NPs hybrids, the concentration of hydrogen peroxide (3.5 ppm) after the first cycle was greater than that of H^+-PAni. However, the concentration of hydrogen peroxide decreased to 0 ppm after the third cycle. However, for H^+-PAni/Ag, Cu, and Ni NPs hybrids, the concentration of hydrogen peroxide after

the first cycle was 1-2 ppm, which was similar to H^+-PAni, and the concentration of hydrogen peroxide was maintained even after the fifth cycle.

Table 11. Concentration of hydrogen peroxide in physiological saline (50 mL).

Cycles	Concentration of hydrogen peroxide (ppm)						
	H^+-PAni NPs	H^+-PAni/Au NPs	H^+-PAni/Pt NPs	H^+-PAni/Pd NPs	H^+-PAni/Ag NPs	H^+-PAni/Cu NPs	H^+-PAni/Ni NPs
1	2	3.5	3.5	3.5	2	1	2
2	1	1	1	0.5	2	1	2
3	0.5	0	0	0	2	1	2
4	0.5	0	0	0	1	1	2
5	0	0	0	0	1	1	2

The same experiments were carried out by using water instead of physiological saline as solvent. The results showed a similar trend to physiological saline (Table 12).

Table 12. Concentration of hydrogen peroxide in water (50 mL).

Cycles	Concentration of hydrogen peroxide (ppm)						
	H^+-PAni NPs	H^+-PAni/Au NPs	H^+-PAni/Pt NPs	H^+-PAni/Pd NPs	H^+-PAni/Ag NPs	H^+-PAni/Cu NPs	H^+-PAni/Ni NPs
1	2	3.5	3.5	3.5	2	1	2
2	1	1	1	1	1	1	2
3	1	0	0.5	0	1	0.5	2
4	0.5	0	0	0	1	1	2
5	0	0	0	0	1	1	2

The UV-Vis-NIR absorption spectra were measured for each electrode film (Figure 19 and 20) to investigate the degradation mechanism after the fifth cycle of the experiments. For the H^+-PAni/Pt NPs hybrid, a peak around 450-500 nm, attributable to a polaron band, decreased significantly compared to the spectra before the generation of hydrogen peroxide. A similar phenomenon was observed for H^+-PAni and H^+-PAni/Au,

Pd NPs hybrids. Dedoping of the *p*-TsOH is considered to be a reason for degradation of the electrode. In addition, a broad peak around 540 nm was observed in the spectrum of the H^+-PAni/Pd NPs hybrid, which was not observed before the generation of hydrogen peroxide. This spectrum is similar to that of the oxidized form of PAni.[33] It suggests that the electrode reduction reaction after oxidation of PAni by molecular oxygen was inefficient. For H^+-PAni/Ag and Cu NPs hybrids, the absorption spectra were similar before and after the generation of hydrogen peroxide, and this was consistent with the results of hydrogen peroxide generation. However, the spectral behavior of H^+-PAni/Ni NPs hybrid was different, though the generation of hydrogen peroxide was maintained. In the spectrum after the fifth cycle, the peak around 330 nm, attributable to the π-π* transition, is the strongest peak in the spectrum. And the absorption at more than 400 nm became smaller than it was before the generation of hydrogen peroxide, although a very broad absorption from 400 to 750 nm was still present. This spectrum is similar to that of the reduced form of PAni.[33] This indicates that the reduction of PAni on the electrode proceeded smoothly in the H^+-PAni/Ni NPs hybrid. This is likely to be a reason why the activity of hydrogen peroxide generation did not decrease for the H^+-PAni/Ni NPs hybrid after the fifth cycle.

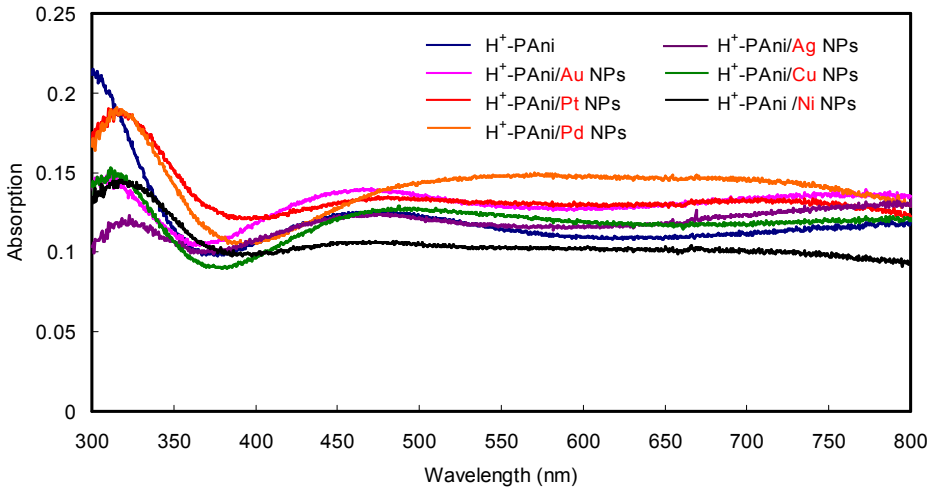

Figure 19. UV-Vis-NIR absorption spectra of the electrode films after the fifth cycle of hydrogen peroxide generation experiments in physiological saline.

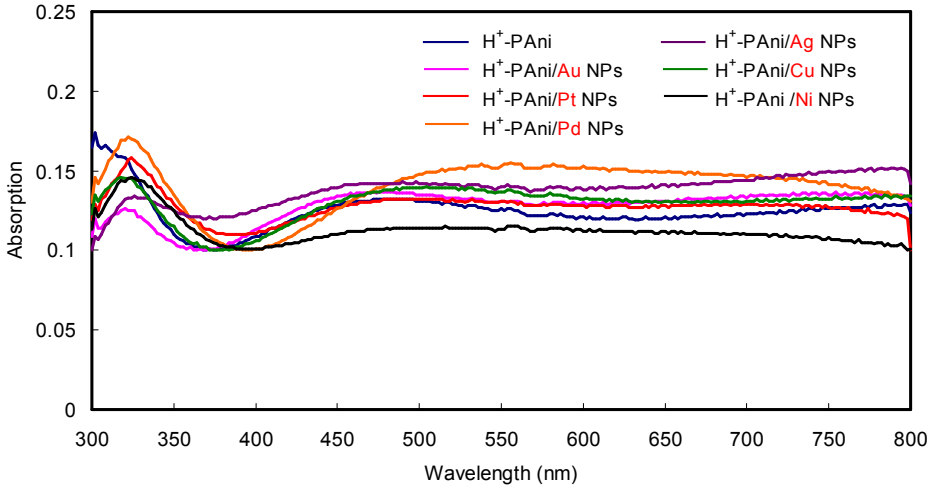

Figure 20. UV-Vis-NIR absorption spectra of the electrode films after the fifth cycle of hydrogen peroxide generation experiments in water.

Conclusion

This study summarizes the preparation and evaluation of H^+-PAni/M NPs hybrids and H+-PAni/M^{n+} complexes (M = Au, Pt, Pd, Ag, Cu, and Ni). H^+-PAni/Ni NPs hybrid showed particularly high conductivity among the H^+-PAni/M NPs hybrids (M = Au, Pt, Pd, Ag, Cu, and Ni). The activity for hydrogen peroxide generation, using H^+-PAni/M NPs hybrids (M = Au, Pt, Pd, Ag, Cu, and Ni) as electrodes, also depended on the metal species. For H^+-PAni/Ag, Cu, and Ni NPs hybrids, an improvement in repetition durability was suggested when compared to H^+-PAni. The UV-Vis-NIR absorption spectra of the electrode films revealed the redox behavior of PAni before and after the reaction. These results are valuable for sterilization applications.

Experimental section

Instrumentation and chemicals

All reagents were purchased from commercial sources and used without further purification. UV-Vis-NIR absorption spectra were recorded on a SHIMADZU UV-VIS-NIR SPECTROMETER UV-3150.

Proton doping

PAni (150 mg), a PAni/M NPs hybrids, or a PAni/M^{n+} complex (M = Au, Pt, Pd, Ag, Cu, and Ni) (150 mg) was dissolved in NMP (10 g). *p*-TsOH was added as dopant (1 equiv per aniline unit of PAni) to the solution. After mixing at room temperature for 1 h, the solvent was removed by evaporation and the material dried *in vacuo* (120 ˚C, 6 h).

Measurement of conductivity

H^+-PAni (50 mg) or a H^+-PAni/M NPs hybrids or a H^+-PAni/M^{n+} complex (M = Au, Pt, Pd, Ag, Cu, and Ni) (50 mg) was pressed to form a pellet (100 kg f/cm^2) and its volume specific resistance (Ω·cm) was measured and used to calculated its conductivity (S/cm).

Preparation of electrode

A 10 wt% solution of DPHA/2-butoxyethanol was added to the H^+-PAni/M NPs hybrids (M = Au, Pt, Pd, Ag, Cu, and Ni) solution to act as a binder. The ratio of H^+-PAni/DPHA (w/w) was 1 : 1. The mixtures were coated onto an ITO/glass substrate (5 cm x 5 cm) by spin coating (500 rpm, 10 s). The film was dried at 150 °C for 1 min, and cured by UV irradiation. The film was cut (5 cm x 2.5 cm) before being used as an electrode.

Hydrogen peroxide generation

Figure 21 shows the equipment used for generating hydrogen peroxide. Physiological saline or water was used as the solvent. The content of hydrogen peroxide in the solvent was measured using semi-quantitative test strips (Quantofix™ Peroxid 25, purchased from MACHEREY-NAGEL). The quantity of solvent used was 50 g, and the applied voltage was set to 2.5 V. The hydrogen peroxide content was measured after applying voltage for 6 h. Then, the electrode was removed from the solvent and dried at room temperature for more than 12 h. This operation was repeated to investigate the repetition durability of the electrode film.

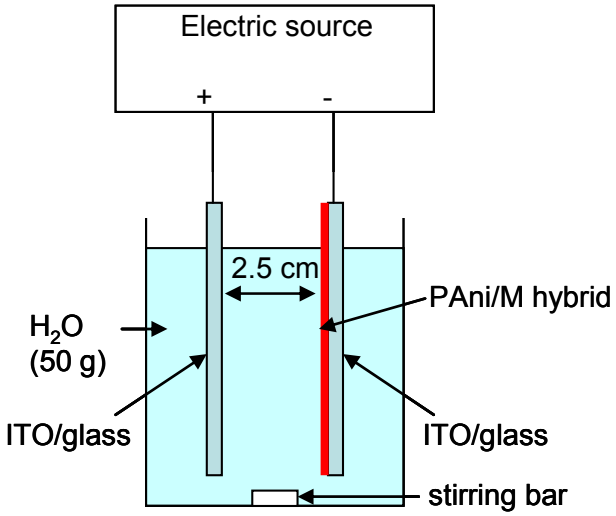

Fig. 21. The equipment for hydrogen peroxide generation.

References

1. A. Drelinkiewicz, M. Hasik, M. Kloc, *J. Catal.* **1999**, *186*, 123.
2. J. Wang, K.G. Neoh, E.T. Kang, *J. Colloid Interface Sci.* **2001**, *239*, 78.
3. T.K. Sarma, D. Chowdhury, A. Paul, A. Chattopadhyay, *Chem. Commun.* **2002**, 1048.
4. S. Sharma, C. Nirkhe, S. Pethkar, A.A. Athawale, *Sens. Actuators B* **2002**, *85*, 131.
5. A.A. Athawale, S.V. Bhagwat, *J. Appl. Polym. Sci.* **2003**, *89*, 2412.
6. J.M. Kinyanjui, R. Harris-Burr, J.G. Wagner, N.R. Wijeratne, D.W. Hatchett, *Macromolecules* **2004**, *37*, 8745.
7. T.K. Sarma, A. Chattopadhyay, *J. Phys. Chem. A* **2004**, *108*, 7837.
8. A. Houdayer, R. Schneider, D. Billaud, J. Ghanbaja, J. Lambert, *Synth. Met.* **2005**, *151*, 165.
9. A. Houdayer, R. Schneider, D. Billaud, J. Ghanbaja, J. Lambert, *Appl. Organometal. Chem.* **2005**, *19*, 1239.
10. R.J. Tseng, J. Huang, J. Ouyang, R.B. Kaner, Y. Yang, *Nano Lett.* **2005**, *5*, 1077.
11. W. Li, Q.X. Jia, H.-L. Wang, *Polymer* **2006**, *47*, 23.
12. K. Mallick, M. Witcomb, M. Scurrell, *Platinum Metals Rev.* **2007**, *51*, 3.
13. B.J. Gallon, R.W. Kojima, R.B. Kaner, P.L. Diaconescu, *Angew. Chem. Int. Ed.* **2007**, *46*, 7251.
14. A. Nyczyk, A. Sniechota, A. Adamczyk, A. Bernasik, W. Turek, Magdalena Hasik, *Eur. Polym. J.* **2008**, *44*, 1594.
15. N.V. Blinova, J. Stejskal, M. Trchová, I. Sapurina, G. Ćirić-Marjanović, *Polymer* **2009**, *50*, 50.
16. A. Nyczyk, M. Hasik, W. Turek, A. Sniechota, *Synth. Met.* **2009**, *159*, 561.
17. A. Drelinkiewicz, A. Zięba, J.W. Sobczak, M. Bonarowska, Z. Karpiński, A. Waksmundzka-Góra, J. Stejskal, *React. Funct. Polym.* **2009**, *69*, 630.
18. S. Ivanov, U. Lange, V. Tsakova, V.M. Mirsky, *Sens. Actuators B* **2010**, *150*, 271.
19. S. Komathi, S. Palaniappan, P. Manisankar, A.I. Gopalan, K.-P. Lee, *Macromol. Chem. Phys.* **2010**, *211*, 1330.
20. R. Liu, H. Qiu, H. Li, H. Zong, C. Fang, *Synth. Met.* **2010**, *160*, 2404.
21. G. Tanami, V. Gutkin, D. Mandler, *Langmuir* **2010**, *26*, 4239.
22. E.A. Sanches, J.C. Soares, R.M. Iost, V.S. Marangoni, G. Trovati, T. Batista, A.C. Mafud, V. Zucolotto, Y.P. Mascarenhas, *J. Nanomater.* **2011**, 1.
23. Y.-F. Huang, Y.I. Park, C.Y. Kuo, P. Xu, D.J. Williams, J. Wang, C.-W. Lin, H.-L. Wang, *J. Phys. Chem. C* **2012**, *116*, 11272.
24. R. Kosydar, M. Goral, A. Drelinkiewicz, *J. Stejskal, Chem. Pap.* **2013**, *67*, 1087.

25. J. Han, J. Dai, C. Zhou, R. Guo, *Polym. Chem.* **2013**, *4*, 313.
26. Z. Li, Y. Li, J. Lu, F. Zheng, J. Laven, A. Foyet, *J. Appl. Polym. Sci.* **2013**, *128*, 3933.
27. D. Zhai, B. Liu, Y. Shi, L. Pan, Y. Wang, W. Li, R. Zhang, G. Yu, *ACS Nano* **2013**, *7*, 3540.
28. A. Liu, L.H. Bac, J.-S. Kim, B.-K. Kim, J.-C. Kim, *J. Nanosci. Nanotech.* **2013**, *13*, 7728.
29. W. Wang, S. Sun, S. Gu, H. Shen, Q. Zhang, J. Zhu, L. Wang, W. Jiang, *RSC Adv.* **2014**, *4*, 26810.
30. L. L. Premvardhan, S. Wachsmann-Hogiu, L. A. Peteanu, D. J. Yaron, P.-C. Wang, W. Wang, A. G. MacDiarmid, *J. Chem. Phys.* **2001**, *115*, 4359.
31. M. Higuchi, D. Imoda, T. Hirao, *Macromolecules* **1996**, *29*, 8277.
32. N. Kawashima, M. Takamatsu, K. Morita, *Colloids and Surfaces B: Biointerfaces* **1998**, *11*, 297.
33. E.T. Kang, K.G. Neoh, K.L. Tan, *Prog. Polym. Sci.* **1998**, *23*, 277.

Conclusions

In this thesis, the synthesis of PAni/M NPs hybrids by two methods was described. From the evaluation of the conductivity and generation of active oxygen in aqueous solutions, the effect of metal species hybridized with PAni was studied.

In Chapter 1, PAni/M NPs hybrids (M = Au, Pt, and Ag) were synthesized from precursor starch/M NPs via the ligand exchange method. The sizes of the M NPs obtained were distributed in a range of diameter of 2-3 nm. Some aggregation was observed in the PAni/Pt and Ag NPs hybrids. Although it is difficult to remove starch completely, this procedure avoids the exposure of the redox-active polymer to the reductant, and is useful for the synthesis of PAni/M NPs hybrids.

In Chapter 2, PAni/M NPs hybrids (M = Au, Pt, Pd, Ag, Cu, and Ni) were synthesized via our template method. The IR spectra suggested that the partial oxidation of the main chain structure of PAni occurred in the complexation step. The partial reduction of the main chain structure of PAni occurred during the reduction of the complexes. In the UV-Vis-NIR absorption spectra of PAni/M NPs hybrids (M = Au, Pt, Pd, Ag, Cu, and Ni) a hypochromic effect in the π-π^* and CT bands was observed. M NPs (mainly in the range of 2-3 nm) were observed in PAni/Au, Pt, and Pd NPs hybrids, but not for PAni/Ag, Cu, and Ni NPs hybrids. However, SEM-EDX images of PAni/M NPs hybrids (M = Au, Pt, Pd, Ag, Cu, and Ni) showed a uniform dispersion of the metals.

In Chapter 3, the preparation and evaluation of the conductivity of H^+-PAni/M NPs hybrids and H^+-PAni/M^{n+} complexes (M = Au, Pt, Pd, Ag, Cu, and Ni) were carried out. H^+-PAni/Ni NPs hybrid showed particularly high conductivity among H^+-PAni/M NPs hybrids (M = Au, Pt, Pd, Ag, Cu, and Ni) and H^+-PAni/M^{n+} complexes (M = Au, Pt, Pd, Ag, Cu, and Ni). The activity for hydrogen peroxide generation, using H^+-PAni/M NPs hybrids (M = Au, Pt, Pd, Ag, Cu, and Ni) as electrode films, depended on the metal species. For H^+-PAni/Ag, Cu, and Ni NPs hybrids, an improvement in repetition durability was observed compared to that of H^+-PAni. The UV-Vis-NIR absorption spectra of the electrode films revealed the redox behavior of PAni before and after the reactions. These results are valuable for sterilization applications.

List of publications

(1) Preparation of Polyaniline/Pt Nanoparticles via Ligand Exchange from Starch/Pt Nanoparticles

Tadayuki Isaji, Toru Amaya, Yuhi Inada, Masashi Abe, and Toshikazu Hirao

Bull. Chem. Soc. Jpn., **2014**, *87* (10), 1130-1132.

(2) Synthesis of Polyaniline and Transition Metal Nanoparticles Hybrids

Toru Amaya, **Tadayuki Isaji**, Masashi Abe, and Toshikazu Hirao

J. Inorg. Organomet. Polym., **2015***, 25* (1), 145-152.

(3) Hydrogen Peroxide Generation Using Polyaniline/Transition Metal Nanohybrid Electrodes

Tadayuki Isaji, Masashi Abe, Toru Amaya, and Toshikazu Hirao

J. Inorg. Organomet. Polym. in press (DOI 10.1007/s10904-015-0172-y).

Acknowledgement

I would like to express my sincerest gratitude to Professor Dr. Toshikazu Hirao, Department of Applied Chemistry, Graduate School of Engineering, Osaka University for his continuous guidance throughout this work and fruitful discussions.

I would like to express deep thanks to Professor Dr. Nobuhito Imanaka and Professor Dr. Hiroshi Uyama, Department of Applied Chemistry, Graduate School of Engineering, Osaka University for reviewing this thesis and their helpful comments.

I would like to express special thanks to Dr. Toru Amaya, Department of Applied Chemistry, Graduate School of Engineering, Osaka University for his frequent helpful advice and hearty encouragement.

Acknowledgement is also made to all members of Professor Dr. Toshikazu Hirao's group for their hearty support, encouragement, and friendship.

Finally, I would like to express my special gratitude to my parents and family for their constant support, encouragement, and understanding.

Tadayuki ISAJI